Materials Research Center
Lehigh University

FINAL REPORT

LONG TERM STABILITY IN THIN FILM FERROELECTRIC MEMORIES

Project Directors: D. M. Smyth
M. P. Harmer

19950619 073

REPORT DOCUMENTATION PAGE

OMB No. 0704-0188

1. AGENCY USE ONLY (Leave blank)	2. REPORT DATE 6/15/95	3. REPORT TYPE AND DATES COVERED APRIL 1, 1991 TO JUNE 30, 1994

4. TITLE AND SUBTITLE

LONG TERM STABILITY IN THIN FILM FERROELECTRIC MEMORIES

5. FUNDING NUMBERS

Grant N00014-91-J-1755

6. AUTHOR(S)

D. M. Smyth
M. P. Harmer

7. PERFORMING ORGANIZATION NAME(S) AND ADDRESS(ES)

Lehigh University
Materials Research Center
Whitaker Lab
5 East Packer Avenue
Bethlehem, PA 18015-3194

8. PERFORMING ORGANIZATION REPORT NUMBER

533644 Final

9. SPONSORING/MONITORING AGENCY NAME(S) AND ADDRESS(ES)

Dr. Wallace Smith - Code 1311
ONR
600 North Quincy Street
Arlington, VA 22217

10. SPONSORING/MONITORING AGENCY REPORT NUMBER

N/A

11. SUPPLEMENTARY NOTES

12a. DISTRIBUTION/AVAILABILITY STATEMENT

Unlimited
~~Copies available upon request~~

This document has been approved for public release and sale; its distribution is unlimited.

12b. DISTRIBUTION CODE

N/A

13. ABSTRACT (Maximum 200 words) The three main goals of the project have been accomplished: 1) a self-consistent model for the defect chemistry of $Pb(Zr_{1/2}Ti_{1/2})O_3$ (PZT) was established, 2) the effect of doping on the degradation of the switchable remanent polarization ("fatigue") was determined, and 3) a field stage for the transmission electron microscope was designed and constructed so that dynamic domain switching can be observed and recorded on video tape. It was determined that the concentration of trapped holes exceeds that of free holes in PZT even at the temperatures of equilibration, and that the hole mobility is thermally-activated. It appears that electron-trapping is also extensive. The ac, bulk conductivity of quenched PZT is dominated by ionic conduction. The transport properties of PZT have been correlated with electron paramagnetic resonance results and theoretical band calculations done elsewhere. Polarization fatigue is enhanced by acceptor-doping, and suppressed by donor-doping in both thinned, bulk samples of $BaTiO_3$ and PZT thin films.

14. SUBJECT TERMS

Thin-films   Ferroelectrics   Defects
Fatigue   PZT

15. NUMBER OF PAGES

42

16. PRICE CODE

17. SECURITY CLASSIFICATION OF REPORT UNCLASSIFIED	18. SECURITY CLASSIFICATION OF THIS PAGE UNCLASSIFIED	19. SECURITY CLASSIFICATION OF ABSTRACT UNCLASSIFIED	20. LIMITATION OF ABSTRACT UNLIMITED

NSN 7540-01-280-5500

Standard Form 298 (Rev. 2-89)

I. SUMMARY

The purpose of this program was to examine the relationship between the defect chemistry of $Pb(Zr_{1-x}Ti_x)O_3$, PZT, with certain electrical properties, particularly the loss of switchable polarization after many ferroelectric switching cycles, commonly called "fatigue". This included a study of the defect chemistry of PZT, a determination of the effects of dopants on fatigue, and the design and construction of an electric field stage so that domain switching could be observed directly in the transmission electron microscope. All of these were successfully accomplished.

The defect chemistry of PZT proved to be considerably more complicated than anticipated, based on the established defect model for the alkaline earth titanates $BaTiO_3$ and $SrTiO_3$. The trapping of holes proved to be important in all of these materials even at equilibration temperatures (500-900°C), and the trapping of electrons is also apparently important in PZT. New experimental techniques had to be developed in order to clarify these added complications. The results correlated very well with work done at Sandia National Laboratories using electron paramagnetic resonance and optical spectroscopy. The so-called "inert pair" of electrons on the Pb^{+2} ion, the two 6s electrons, clearly have a strong influence on the properties of the lead-based systems.

As expected, doping has a strong effect on polarization fatigue. It was demonstrated that acceptor dopants reduced the fatigue life, while donor dopants increased it. This is in accord with the fact that the oxygen vacancy concentration is increased by acceptor doping, and decreased by donor doping. However, the results do not distinguish between the transport of oxygen vacancies or of trapped holes as the deleterious migrating species, since for the same equilibration conditions, the trapped hole concentration will increase with increasing oxygen vacancy concentration. It has recently been shown at Sandia that fatigued samples can be restored to their unfatigued state by optical illumination, and this suggests that the movement of holes is at least a major contributing factor to fatigue.

In the third phase of the program, an electric field stage for the transmission electron microscope was constructed to our specifications by Gatan, Inc. After a few modifications, direct observation of domain switching was achieved. The results have been stored on video tape and were demonstrated at several international symposia. However, it has proved to be very difficult to mount the electroded samples with electrical connections in the field stage. The samples break very easily, and the yield of successful experiments is small.

1

Availability Codes

| Dist	Avail and/or Special
A-1	

II. THE DEFECT CHEMISTRY OF PZT

A. Experimental Results and the Defect Model

It was initially anticipated that the defect chemistry of PZT would be essentially identical with the established model for the alkaline earth titanates such as $BaTiO_3$ and $SrTiO_3$ (1-5). However, three new aspects of the defect behavior were discovered. First, it was realized that the existing model for the perovskite titanates was incomplete in that it ignored the trapping of holes under equilibrium conditions. This was always a bit of a puzzle, because hole-trapping near room temperature is an essential requirement for the observed insulating properties of these materials. The acceptor trap depth necessary to achieve this behavior should be large enough to insure substantial trapping even at equilibration temperatures up to 1000°C, but the model seemed to work very well with the assumption that hole-trapping is negligible at those temperatures. However, Waser has since demonstrated that major amounts of hole-trapping can be included in the model without destroying its basic features (6). This still needed to be verified experimentally since the usual equilibrium conductivity measurements are blind to this phenomenon. The second difference is that the hole mobility in PZT is thermally-activated, whereas the hole conduction in the alkaline earth titanates appears to be band-type, and there is no evidence for thermal activation (5). This different behavior for hole transport in PZT is attributed to the different electronic structure of the Pb^{+2} ion, as will be discussed. Finally, there is strong evidence for significant electron-trapping in reduced and in donor-doped PZT. This is completely different from the behavior of $BaTiO_3$ and $SrTiO_3$ where electron transport is clearly by band conduction.

The older defect model for the perovskite titanates was based on measurements of the equilibrium electrical conductivity as a function of temperature and oxygen activity, $P(O_2)$. The results of such measurements on $BaTiO_3$ and PZT are shown in Figs. 1 and 2. [All of our PZT samples had the composition $Pb(Zr_{1/2}Ti_{1/2})O_3$]. Only the p-type behavior at high values of $P(O_2)$ are shown for PZT; the behavior under more reducing conditions will be discussed later. In the p-type region, the behavior is seen to be very similar with a log slope of +1/4. These results were fit to a reduction reaction

$$(1) \qquad O_0 \rightleftharpoons 1/2 O_2 + V_0^{\cdot\cdot} + 2e'$$

and an oxidation reaction

(2) $$1/2 O_2 + V_O^{\cdot\cdot} \rightleftharpoons O_O + 2h^{\cdot}$$
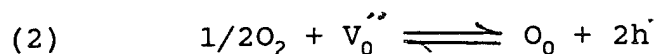
The reduction reaction is straightforward; it leads to the formation of oxygen vacancies, a well-established defect, and electrons, which are favored in these compounds because of the presence of the reducible cation Ti^{+4}. However, the oxidation reaction requires an extrinsic source of oxygen vacancies, due to either naturally-occurring or deliberately-added acceptor impurities, or cation nonstoichiometry such as a deficiency of PbO in PZT. Otherwise, oxidation would be expected to be extremely difficult, because of the absence of an oxidizable species (except in the case of Pb^{+2}) and the unfavorable nature of the intrinsic lattice defects formed by oxidation, either oxygen interstitials or A- or B-site vacancies. The presence of extrinsic oxygen vacancies gives an easy mechanism for the incorporation of a stoichiometric excess of oxygen without requiring a crystallographic excess. In no case observed to date has the stoichiometric excess of oxygen been sufficient to consume all of the extrinsic oxygen vacancies in acceptor-excess material.

The enthalpies of the oxidation and reduction reactions were obtained from the temperature dependences of the equilibrium conductivities in the appropriate regions (1,2). In $BaTiO_3$ the enthalpy of reduction is 5.90 eV, and the enthalpy of oxidation is 0.92 eV. The low value for the latter reflects the ease of accommodating the excess oxygen in the lattice. The algebraic sum of Eqs. (1) and (2) gives twice the intrinsic ionization reaction

(3) $$nil \rightleftharpoons e' + h^{\circ}$$
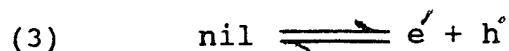
Thus the band gap at 0 K for $BaTiO_3$ (or enthalpy of intrinsic ionization) should be (5.90 + 0.92)/2 = 3.41 eV, and this is confirmed from the temperature dependence of the conductivity minima. This indicates that there is no temperature dependence for the concentration of oxygen vacancies near the conductivity minima, and this is expected since they result from an extrinsic source. This model was also found to be consistent with the results of thermopower measurements (5). It is summarized in a schematic diagram shown in Fig. 3.

The problem with the model just described is that hole traps at least 0.5 eV deep are required to explain the insulating behavior of these materials near room temperature. But the value of the term $exp(-0.5/kT)$ at 800°C is 0.005, indicating a comparably small fractional ionization of the trapped holes even under equilibration conditions. Waser showed that this can be incorporated into the original model without distorting its essential features (6). This led to the defect diagram shown in Fig. 4, where it is seen that the major hole species produced by oxidation is the trapped hole,

3

and that it also has a log slope of +1/4. This means that the main oxidation reaction is

$$(4) \qquad 1/2 O_2 + V_O^{\cdot\cdot} + 2A' \rightleftharpoons O_O + 2A^x$$
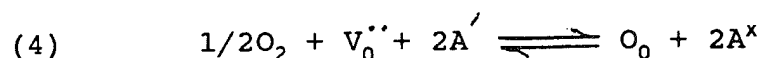
where A' is a charged acceptor center, and A^x is an acceptor center with a trapped hole. Thus Eq. (1) is the oxidation reaction to form free holes, whose enthalpy is determined by the temperature dependence of the equilibrium conductivity, while Eq. (4) is the oxidation reaction to form trapped holes. The two oxidation reactions are linked by the ionization reaction

$$(5) \qquad A^x \rightleftharpoons A' + h^{\cdot}$$
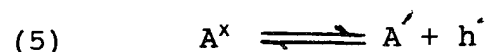
If the enthalpy of either the ionization reaction, or of the oxidation reaction to form trapped holes can be determined, the other enthalpy can be obtained with the help of the enthalpy of oxidation to form free holes, which is known.

A way to measure the enthalpy of oxidation to form trapped holes was developed. It is based on the mass-action expression for Eq. (4), solved for the equilibrium $P(O_2)$.

$$(6) \qquad P(O_2) = \{[O_O]/K_{ox}[V_O^{\cdot\cdot}]\}^2 \{[A^x]/[A']\}^4 \exp(2\Delta H_{ox}/kT)$$

If the equilibrium oxygen activity, $P(O_2)$, can be measured as a function of temperature while keeping all of the other terms unchanged, then the enthalpy of Eq. (4), ΔH_{ox}, can be determined directly. The only term that might vary is $[A^x]$, the concentration of trapped holes. If the experiment is carried out in a sealed cell, as shown in Fig. 5, with a large sample mass, and a very small gas volume, then the amount of oxygen that must enter or leave the sample to maintain equilibrium can be relatively small. In our experiments, it was estimated that $[A^x]$ was kept constant to better than 1%.

As shown in Fig. 5, the components of the cell are hermetically sealed together by means of glass gaskets that soften and deform in the experimental temperature range. The lid is a disk of yttria-doped zirconia, with platinum electrodes on both sides, that serves as an electrochemical oxygen sensor. The oxygen activity inside the cell is determined from the emf of the oxygen concentration cell by means of the Nernst equation

$$(7) \qquad E = [RT/4F]\ln[P(O_2)'/P(O_2)'']$$

where F is the Faraday constant, $P(O_2)$ is the activity inside the cell and $P(O_2)$ is the activity in the surrounding air. Results for PZT are shown in Fig. 6. If hole-trapping were negligible, the enthalpy determined from this experiment should be similar to that obtained from the equilibrium conductivity, which is 0.74 eV. However, the enthalpy determined by the constant concentration experiment not only does not have the same numerical value, it is even of opposite sign, -0.49 eV. This a clear indication that hole-trapping is indeed of major importance.

Additional experiments are necessary in order to obtain all of the pertinent thermodynamic parameters. This is particularly true because of a previous report that the hole mobility in PZT is thermally-activated (7). Two additional experimental techniques were used in this study. The first is measurement of the thermoforce (Seebeck coefficient) as a function of temperature under equilibrium conditions. The second is the measurement of the equilibrium conductivity as a function of temperature under conditions of constant composition in the sealed cell.

Results of the thermoforce measurements are shown in Fig. 7. It is seen that the composite enthalpy depends on the value of $P(O_2)$ with which the sample was equilibrated during the experiment. This is caused by the substantial contribution to the thermoforce made by electrons well into the p-type region. In order to avoid this problem, the measurements shown in Fig. 7 were made on a heavily acceptor-doped sample in order to move the p-n transition to as low a $P(O_2)$ as possible. The composite enthalpy seems to be drifting toward that obtained for $P(O_2)$ = 1 atm, which was taken as the best value. The thermoforce is directly related to the carrier concentration, except for as additive transport factor. Fortunately that factor is zero for small polaron conduction, which appears to be the case for PZT. The fact that the apparent enthalpy for oxidation to form free holes, obtained from the equilibrium conductivity measurements, is larger than the enthalpy for the carrier concentration, obtained from the thermoforce measurements, indicates that there is an enthalpy for the hole mobility, i.e. it is thermally-activated.

The measurement of the equilibrium conductivity at constant composition requires a more complex sealed cell in order to connect all of the electrical leads. A schematic diagram of the cell used in our experiments is shown in Fig. 8. In order to keep all of the cell components properly aligned, the stack was enclosed in an outer alumina tube whose ID was only slightly larger than the cell OD. The system was flooded with a gas having the desired $P(O_2)$, and when the experimental temperature was reached, the assembly was gently pressed together with a push-rod in order to achieve a hermetic seal. The glass gaskets were chosen to soften in the desired temperature range, and their softening range limited the temperature excursion of the experiment. The successful achievement of a hermetic seal was indicated by the reversibility of the measurements. Since the gaskets cracked when the cell was

cooled to room temperature, each experiment required a new cell assembly. The results of such an experiment are shown in Fig. 9.

All of these experiments give different combinations of enthalpy terms as shown in Table I for PZT. These lead to the individual enthalpies shown in Table II. (Both Tables are on the following page.) There are three independent enthalpies, and four sets of their combinations, so the results are over-determined by one relationship. It is comforting to see that the same values are obtained from different combinations of the experimental results.

Because of the importance of the concept of hole-trapping at the equilibration temperatures, constant composition measurements have also been performed on $BaTiO_3$, $SrTiO_3$, and $CaTiO_3$ as part of a separately supported project. The results were similar and confirmed that in all of these compounds, trapped holes are the major hole species that result from a stoichiometric excess of oxygen.

B. Practical Implications

The amount of excess oxygen in oxidized samples is directly proportional to the concentration of excess hole species. The concentration of trapped holes exceeds that of free holes, as determined from equilibrium conductivity and thermoforce measurements, and therefore, the amount of excess oxygen is larger than previously thought.

The negative enthalpy of oxidation to form trapped holes indicates that the concentration of trapped holes, and hence of excess oxygen, increases with _decreasing_ temperature, the opposite of the deduction made from the conductivity measurements alone. The equilibrium conductivity increases with increasing temperature because of an increasing ionization of a decreasing population of trapped holes. The trapped hole concentration decreases with increasing temperature with an activation enthalpy of $\Delta H_{ox}/2 = -0.79/2 = -0.40$ eV, while their fractional ionization increases as the trap depth, +0.70 eV. Early attempts to measure the amount of excess oxygen by thermogravimetry focused on the highest possible temperatures in the misguided opinion that this was the region of highest nonstoichiometry. It is now apparent that that is the wrong direction.

The concentration of trapped holes in quenched samples is not just the concentration of free holes under equilibrium conditions, but is the sum of all hole species, essentially the trapped hole concentration, a much larger number. This has implications for fatigue if the migration of trapped holes is a significant factor, as now seems likely.

At room temperature, the transition from a p-type insulator, for

TABLE I.   Summary of Arrhenius Analysis Results for the Various Equilibrium Techniques

Technique	Thermodynamic Parameters	Enthalpy
Equilibrium Cond.	$\Delta H_{ox}/2 + E_A + \Delta H_M$	0.74 eV
Thermopower	$\Delta H_{ox}/2 + E_A$	0.45
Const. Comp. $P(O_2)$	ΔH_{ox}	-0.49
Const. Comp. Cond.	$E_A + \Delta H_M$	0.98

TABLE II.   Thermodynamic Parameters for Defect Formation and Electronic Transport in PZT

ΔH_{ox}	E_A	ΔH_M
-0.49 eV	0.70 eV	0.29 eV

samples equilibrated at high $P(O_2)$, to an n-type semiconductor, for samples equilibrated at low $P(O_2)$, does not occur at the equilibrium conductivity minima, which are defined by the intersection of the concentration of free electrons with that of free holes. It occurs at the intersection of all electron species with all hole species. In the case of $BaTiO_3$, this corresponds to the intersection of free electrons with trapped holes, and this occurs far below the conductivity minima. This explains why the Japanese manufacturers of multilayer ceramic capacitors with base-metal electrodes, e.g. nickel, can fire their capacitors in H_2-N_2 mixtures and still retain an insulating dielectric. This would have been much too reducing if the insulator-semiconductor transition corresponded to the conductivity minima.

C. Charge Transport in Quenched Samples

While equilibration at elevated temperatures establishes the state of nonstoichiometry and the general levels of defects, charge transport in quenched samples at lower temperatures is of much more interest for applications. An example of such measurements for $BaTiO_3$, made for another project, is shown in Fig. 10. Samples were equilibrated at either 800 or 1000°C in various $P(O_2)$s, and then quenched by rapid withdrawal from the hot zone of the furnace. Conductivities were then measured in the range 250-350°C by ac impedance analysis. At these temperatures, the conductivities were still high enough to measure conveniently, but equilibration times were slow enough to avoid any compositional changes during the measurements. The impedance analysis technique was used to obtain bulk values of the conductivity, by excluding the effects of electrode interfaces and grain boundaries.

For equilibration at the highest $P(O_2)$ values, the log slope is +1/4 with an activation energy of about 0.7 eV. These are both charactersistic of oxygen-excess p-type conductivity, with the activation energy corresponding closely to the measured depth of the hole traps. At lower values of $P(O_2)$ the conductivity is independent of $P(O_2)$ and has an activation energy of about 1 eV. These correspond to what is expected for oxygen vacancy conduction, with the activation energy being attributed to the enthalpy of motion of the vacancies. The increased prominence of ionic conduction in the low temperature range is caused by the more rapid drop of the electronic conductivity minimum, which has an activation energy of half the band gap, $3.4/2 = 1.7$ eV, than that of the ionic conductivity, which has an apparent activation energy equal to the enthalpy of motion, about 1 eV. It should be recalled that these are ac measurements. Under dc conditions, this ionic component would be expected to rapidly polarize. At the lowest values of $P(O_2)$ the conductivity rises abruptly, indicating that the transition from the insulating to the semiconducting state has occurred. Note that this transition occurs at $P(O_2)$ values far below those at the conductivity minima, in accord with the preceding discussion of the influence of trapped holes.

Similar results are shown for PZT in Fig. 11. In this case there

8

is no observable p-type region at high $P(O_2)$, but there is a long plateau with an activation energy of about 1 eV that is assumed to be ionic conduction. Below about 10^{-14} atm, the conductivity rises rapidly with further reduction, as would be expected for n-type conductivity. There are several points of interest in this region. First of all, the conductivity levels are an order of magnitude or more lower than the values measured at the equilibration temperature of 700°C. Secondly, there is a distinct temperature dependence for the quenched conductivity, with an apparent activation energy of about 1 eV. Both of these observations would be consistent with the localization of the electrons in fairly deep traps. Further information has been obtained by measurement of the equilibrium oxygen activity as a function of temperature at constant defect concentrations in the presumed n-type region, using the sealed cell technique. The results are shown in Fig. 12. The measured enthalpy, 2.8 eV, is very low compared with the enthalpies of reduction for $BaTiO_3$ and $SrTiO_3$, e.g. 5.90 eV for the former. This suggests that the electrons are trapped, rather than being required to be at higher energies in the conduction band. Thus the measured enthalpy is most likely that for reduction with the formation of trapped electrons

$$(8) \qquad O_0 + 2Ti_{Ti} \rightleftharpoons 1/2O_2 + V_O^{\cdot\cdot} + 2Ti_{Ti}'$$

where it has been assumed that the electrons are trapped on Ti ions in the form of Ti^{+3}. An estimate of the electron trap depth, E_D, can be obtained by combination of the enthalpies of oxidation with the formation of trapped holes, Eq. (4), the ionization of trapped holes, Eq. (5), reduction with the formation of trapped electrons, Eq. (8), and ionization across the band gap, Eq. (3). This gives the relationship

$$(9) \qquad E_D = E_g - E_A - (\Delta H_{ox} + \Delta H_{red})/2$$

where ΔH_{red} is the enthalpy of Eq. (8). If the band gap, E_g, is taken to be about 3.1 eV then this gives an apparent electron trap depth, E_D, of about 1.2 eV. This is in reasonable agreement with the theoretical calculations of Robertson (8), which indicate the Ti^{+4} should be a deep electron trap, probably more than 1 eV below the conduction band. Combination of the reduction reaction with the formation of trapped electrons, and the ionization reaction for the trapped electrons, yields an enthalpy of reduction with formation of free holes of 5.3 eV in PZT, and this is reasonably close to the values found for the alkaline earth titanates. While each bit of evidence for significant electron-trapping in PZT is rather circumstantial, taken as a whole they make a rather convincing case. This represents a significant difference from the behavior of electrons in the alkaline earth titanates. It also suggests that there is no semiconducting behavior in PZT, but that it is an insulator regardless of the equilibration conditions.

9

These results indicate that the defect diagram for PZT may have to be modified as shown in Fig. 13. The final thing to be noted about the data is that the $P(O_2)$ dependence of the conductivity in the presumed n-type region is approximately linear, which is much too steep to be explained by any straightforward defect model.

D. Pb^{+3} and Ti^{+3} Centers

The transport properties that we have observed for PZT correlate very well with experimental observations of Warren at the Sandia National Laboratories, and the theoretical calculations of Robertson at Cambridge University. Warren has observed by electron paramagnetic resonance that after PZT has been illuminated with band gap light there are distinct signals for Pb^{+3} and Ti^{+3} centers (9). These centers are stable at cryogenic temperatures, e.g. 25 K, but decay within a few hours at room temperature. The Pb^{+3} center can be attributed to the specific electronic structure of the Pb^{+2} cation. This is one of the three so-called "inert pair" cations, the others being the bracketing cations Tl^{+1} and Bi^{+3}. In all of these cations, the two 6s electrons are retained by the ion. These electrons are usually located in a directional orbital that influences the structure of their compounds. The existence of these electrons makes possible the trapping of a hole, the equivalent of the loss of one of these electrons. (It is interesting to note that all three of these "inert pair" cations are important components of many of the high T_c superconducting cuprates, along with the cation of the preceding element, $(Hg_2)^{+2}$, which has the equivalent of an "inert pair" of electrons, although they are located on a diatomic cation. Obviously these electrons have a strong influence on the electronic properties of the compounds of these cations.) In the alkaline earth titanates, the cations, e.g. Ba^{+2} and Sr^{+2}, have the closed shell rare gas electronic structure, and the removal of additional electrons, i.e. the trapping of a hole, is energetically prohibitive.

Theoretical calculations by Robertson indicate that the top of the valence band in PZT is about equally divided between Pb 6s and O 2p character (8). Apparently in the presence of a hole, the Pb 6s states can be lifted into the gap to form a shallow hole trap. After illumination, which ionizes electrons and holes across the gap and also ionizes holes from the deep, stable traps, both carriers start to look for lower energy states. Since there are Pb^{+2} and Ti^{+4} cations in every unit cell, these are usually the first traps seen by both carriers. At higher temperatures, the holes in the Pb^{+3} centers can decay by recombination with the electrons in the Ti^{+3} centers, or by dropping back into the deep, stable traps represented by acceptor centers. With two modes of decay for the Pb^{+3}, but only one for the Ti^{+3}, it is to be expected that the former will decay more rapidly, as is observed. The ability of the Pb^{+2} ions to serve as shallow hole traps is consistent with the thermally-activated hole mobility observed in PZT. Hole conduction apparently occurs by trap-mediated hopping between Pb cations.

The calculations by Robertson also indicated that Ti^{+4} should behave

10

behave as a deep electron trap, with levels 1 eV or more below the conduction band. This accounts for the Ti^{+3} centers, and for the apparent trapping of electrons in PZT equilibrated in reducing atmospheres. There are no comparable centers in the alkaline earth titanates. If they are so deep, why aren't the Ti^{+3} centers more stable? It is because PZT normally has a net acceptor excess due to its natually-occurring impurity content or to loss of PbO. Thus in these samples, the Ti^{+3} centers exist with an excess of trapped holes and eventually disappear by recombination. This suggests that Ti^{+3} should be stable in the n-type region. Indeed, Warren has observed stable Ti^{+3} at room temperature in PLZT, which is PZT that is donor-doped with La^{+3}, and hence has an excess of electron states (10). Thus there are left-over Ti^{+3} centers after all of the photo-induced Pb^{+3} centers have been consumed by recombination.

III.   THE EFFECT OF DOPING ON POLARIZATION FATIGUE

Fatigue in ferroelectric nonvolatile memories is defined as the loss of switchable polarization after repeated switching cycles. Eventually the loss becomes so great that the sense circuit can no longer distinguish between a switching and a nonswitching pulse, and the memory effect is lost. In practice, devices are expected to withstand 10^{12}, or even 10^{15} switching cycles during their useful life. In PZT, serious fatigue often begins after about 10^8-10^{10} cycles, although significant improvement has been achieved by the use of conducting oxide electrodes, e.g. RuO_2 or $La_{1-x}Sr_xCoO_3$, rather than platinum.

It has long been known that ferroelectric ceramic capacitors degrade under temperature-voltage stress due to the migration of oxygen vacancies. The elegant work of Waser has given detailed information on this process (11,12). The capacitors are normally subjected to fields of the order of 10^4 v/cm. The thin film ferroelectric memories are typically switched with fields of about 5×10^5 v/cm, about a factor of 50 higher than the fields applied to the capacitors. This is close to the fields with which the valve metals are anodically oxidized to grow thin dielectric films for electrolytic capacitors. In that case, ionic currents of the order of milliamps per cm^2 flow through the films. At these fields, the conductivity is no longer ohmic, and the ionic current depends exponentially on the applied field. Thus it is clear that with the fields used to switch the nonvolatile memories, oxygen vacancies can be expected to be mobile. In the previous section it was shown that the conductivity of PZT near room temperature contains a large ionic component.

Based on the preceding arguments, it was postulated that polarization fatigue results from the migration of oxygen vacancies. Their redistribution could result in nonuniform electrical fields within the films, or the vacancies might preferentially locate at domain walls, hindering their movement. If the migration of vacancies is the source of the problem, it

11

should be very sensitive to impurity doping, since that strongly affects the oxygen vacancy concentration. Acceptor-dopants, which are cations that have a smaller charge than the ion they replace, bring less oxygen per cation into the structure, and are compensated by oxygen vacancies

$$(10) \qquad A_2O_3 \xrightarrow{(2TiO_2)} 2A'_{Ti} + 3O_O + V_O^{\cdot\cdot}$$
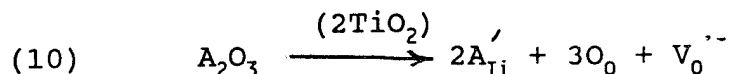
Where A_2O_3 is the oxide of a generic trivalent cation, A^{+3}, that substitutes for Ti^{+4} in the lattice. It is to be understood that A_2O_3 replaces the amount of TiO_2 shown in parentheses above the reaction arrow. It is seen that acceptor-doping increases the oxygen vacancy concentration.

Donor-dopants have a greater charge than the ion they replace, and thus attempt to bring more oxygen into the structure. For donor concentrations less than about 0.5 atom % in $BaTiO_3$, the excess oxygen is expelled even when the material is processed in air, leaving behind electrons as the compensating species

$$(11) \qquad D_2O_5 \xrightarrow{(2TiO_2)} 2D_{Ti}^{\cdot} + 4O_O + 1/2O_2 + 2e'$$
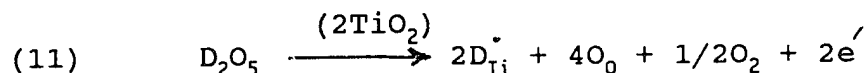
where D_2O_5 is the oxide of a generic pentavalent cation, D^{+5}, that substitutes for Ti^{+4}. This results in semiconducting properties that are of no interest for the applications with which we are concerned. For higher donor concentrations in $BaTiO_3$, there is a change of compensation mechanism, the excess oxygen is retained, and the major compensating defect is the Ti vacancy (13)

$$(12) \qquad 2D_2O_5 + 5BaO \xrightarrow{(4TiO_2)} 5Ba_{Ba} + 4D_{Ti}^{\cdot} + V_{Ti}^{''''} + 15O_O$$
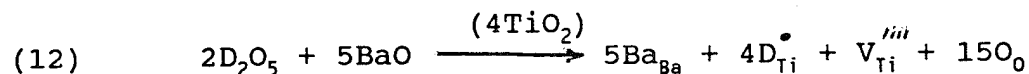
This mechanism gives insulating properties, and appears to be the mode of donor incorporation in oxidizing atmospheres for the other perovskite titanates. Since the donor centers bear a positive defect charge, the positively charged oxygen vacancies are substantially suppressed by their presence.

Thus if oxygen vacancies are the major contributors to fatigue, the acceptor-doping should increase the rate of fatigue, while donor-doping should delay it. This hypothesis has been tested on both thinned $BaTiO_3$ ceramics and on thin film PZT, prepared by the spin-on sol-gel process. $BaTiO_3$ was used to avoid the complication of PbO-loss, hence giving a clearer control of all of the defect species. The sintered $BaTiO_3$ samples were cut, ground, and polished to thicknesses of about 150-250 μm, and evaporated gold electrodes were applied. A unipolar switching field of about 30 kV/cm was applied with a frequency of 100-800 Hz. The results are shown in Fig. 14 in the form of the remanent polarization, measured

at 100 Hz, vs. the number of switching cycles. The undoped samples are known to contain some hundreds of ppm of net acceptor excess from natural sources. The 0.1 % Al doping should moderately increase the oxygen vacancy content. The 2 % Ca doping was compositionally adjusted so that the Ca^{+2} would substitute for Ti^{+4}, where it acts as an acceptor (14). This is a strongly acceptor-doped composition, and the oxygen vacancy concentration should be strongly enhanced. 3 % Nb represents a heavy donor-doping and the oxygen vacancy concentration should be severely suppressed. The results are generally in line with expectations. The donor-doped sample is clearly the most stable, while the heavily acceptor-doped sample degrades the fastest. The undoped and lightly acceptor-doped samples lie in between these extreme behaviors.

Similar results for PZT thin films are shown in Fig. 15. The PZT films were made from three spun-on layers and were about 230 nm thick. The fatigue test was performed with bipolar switching pulses of 430 kV/cm with a frequency of 50-200 kHz. Two samples are shown, one of undoped PZT, the other of PNZT which contained 5 % Nb as the donor-dopant. Once again, the donor-doped sample was more stable than the undoped sample, although the distinction is not as dramatic as in the case of the thinned $BaTiO_3$ samples. This is most likely due to less accurate control of the defect concentrations due to the uncertainty of the amount of PbO lost during processing. Although the compositions were compounded with 5% excess PbO, there is undoubtedly some loss.

Control of the PbO content is essential for the effectiveness of the donor-dopants in PZT. The oxygen vacancies that result from the loss of PbO

$$(13) \qquad Pb_{Pb} + O_O \rightleftharpoons PbO + V_{Pb}'' + V_O^{\cdot\cdot}$$
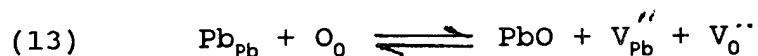
can accomodate some or all of the excess oxygen associated with the donor dopant. Then the lead vacancies effectively serve as the compensating defect, and the effect of the donors is reduced. If the PbO-loss exceeds the donor concentration, then the materials act as excess acceptor-doped material, and the donor is totally ineffective. This is shown schematically in Figs. 16 and 17, which show the effect of increasing donor concentration on the oxygen vacancy concentration for two cases. In the first case, Fig. 16, the amount of PbO-loss is held below the background acceptor impurity content. As the donor concentration exceeds the acceptor content the oxygen vacancy content is strongly suppressed. In Fig. 17, the PbO-loss exceeds the background acceptor content. The oxygen vacancy concentration starts out at a higher level, and it requires much higher donor concentrations to obtain comparable suppression of the oxygen vacancy concentration. In fact the required donor concentration can easily exceed its solubility limit. Thus it is absolutely vital to control the PbO content in order for donor-doping to be effective in improving the fatigue life.

It has recently been determined by Warren at the Sandia National Laboratories that fatigued thin films of PZT can be rejuvenated by photoexcitation (10). This is incompatible with the hypothesis that fatigue is primarily due to the migration of oxygen vacancies. However, this does not alter the expectations for the effects of doping. For equivalent equilibration under oxidizing conditions, the concentration of trapped holes will increase with the concentration of extrinsic oxygen vacancies, and hence with the acceptor content. Thus the observation that fatigue is faster in acceptor-doped samples, and slower in donor-doped samples, does not distinguish between oxygen vacancies and trapped holes as the critical mobile species. It is possible that both make a contribution that may depend on the precise composition and processing conditions.

IV.   THE OBSERVATION OF DOMAIN-SWITCHING BY ELECTRON MICROSCOPY

To study the effect of an external applied electrical field on the domains and the interaction of domains with microstructure, a special stage for the transmission electron microscope (TEM) was designed and constructed. The stage was initially constucted by Gatan Inc.,and was subsequently modified as experience indicated preferred configurations for ease of operation. Schematic diagrams of the TEM stage and the electrode configuration used in this study are shown in Figs. 18 and 19. Platinum wires were bonded onto an insulating alumina ring using silver paste, and the ring was placed in the bottom of the TEM stage. The Pt wires were then connected to the external leads. Gold electrodes (42 μm spacing) were evaporated onto the surface of the specimen. In this configuration, the applied electric field is along the surface of the specimen and normal to the incident electron beam. The microscopy was performed with a Philips 400T electron microscope, operated at 120 kV and equipped with a CCD camera. The images were recorded on video tape with a VCR.

Results obtained from preliminary experiments were conducted on Fe-doped and undoped $BaTiO_3$ single crystals. The magnitude of the applied field had to exceed a critical value before domain-switching occurred. For the undoped $BaTiO_3$ sample, the critical field for domain-switching was approximately 5 kV/cm. Only the domains oriented along the direction of the applied field appeared to switch, while the domains oriented normal to the applied field did not switch even in the presence of fields stronger than the critical field. In addition, not all domains oriented along the field moved to the same extent or with the same velocity. When domains oriented parallel to the field direction intersected with domains normal to the field, the growth of the domain ceased. In some cases, the intersecting domain was pinned and could not be switched back to its original state (either by removing the field or by applying a field of opposite polarity). In the Fe-doped specimen, the field required to switch a given set of domains

increased with repeated switching of the domains. In the case of polycrystalline $BaTiO_3$, the domains did not appear to switch even in the presence of applied fields greater than 100 kV/cm. Possible reasons are the pinning of the domains by the grain boundaries or other local effects on the specimen surface that may result in a nonuniform field across the contacts.

In general, the switching behavior was very discontinuous. As the critical field was approached, the leading edge of the domains became very nervous, with a great deal of rapid jittering back and forth with small amplitude oscillations. The domain then moved very rapidly to a new position, and the process started over again. The dynamics of the switching behavior can only be appreciated by observing the video tapes. Copies are available to anyone who wishes to study the effects personally. The results have been demonstrated at several scientific conferences (see the references to Chen, Harmer, and Smyth; Saikumar, Harmer, and Smyth; and Saikumar, Chan, and Harmer in the list of presentations, Section VI).

The biggest problem with this experiment is the fragility of the specimens. They must be thinned until they are transparent to the electron beam, and it is then difficult to connect them into the electrical circuit without breakage. The yield of acceptable samples is very small, and this reduced the number of specimens that could be studied.

V. REFERENCES

1. N.-H. Chan, R. K. Sharma, and D. M. Smyth, J. Am. Ceram. Soc. 64 [9], 556 (1981).

2. N.-H. Chan, R. K. Sharma, and D. M. Smyth, J. Am. Ceram. Soc. 65 [3], 167 (1982).

3. N.-H. Cham and D. M. Smyth, J. Am. Ceram. Soc. 67 [4], 285 (1984).

4. N.-H. Chan, R. K. Sharma, and D. M. Smyth, J. Electrochem. Soc. 128 [8], 1762 (1981).

5. G. M. Choi, H. L. Tuller, and D. Goldschmidt, Phys. Rev. B 34 [10], 6972 (1986).

6. R. Waser, J. Am. Ceram. Soc. 71 [1], 58 (1988).

7. V. V. Prisedsky, V. I. Shishkovsky, and V. V. Klimov, Ferroelectrics 17, 465 (1978).

8. J. Robertson, W. L. Warren, B. A. Tuttle, D. Dimos, and D. M. Smyth, Appl. Phys. Letters 63 [11], 1519 (1993).

9. W. L. Warren, C. H. Seager, D. Dimos, and E. J. Friebele, Appl. Phys. Letters 61, 2530 (1992).

10. W. L. Warren, private communication.

11. R. Waser, T. Baiatu, and K. H. Hardtl, J. Am. Ceram. Soc. 73, 1645 (1990).

12. R. Waser, T. Baiatu, and K. H. Hardtl, J. Am. Ceram. Soc. 73, 1654 (1990).

13. H. M. Chan, M. P. Harmer, and D. M. Smyth, J. Am. Ceram. Soc. 69 [6], 507 (1986).

14. Y. H. Han. J. B. Appleby, and D. M. Smyth, J. Am. Ceram. Soc. 70 [2], 96 (1987).

VI. PERSONNEL

Program Directors: D. M. Smyth, Paul B. Reinhold Professor of Materials Science and Engineering, and Professor of Chemistry.

M. P. Harmer, Alcoa Foundation Professor of Materials Science and Engineering, and Director of the Materials Research Center.

Postdoctoral Research Associates:

Dr. Jie Chen, now at Hewlett-Packard Co. in Andover, MA

Dr. V. Saikumar

Doctoral Candidates:

Mark V. Raymond, now at Sandia National Laboratories

Chen-hui Jiang, supported by employer

VII. PRESENTATIONS RELATED TO THIS PROGRAM

A. Invited

D. M. Smyth, "Recent results on the defect chemistry of ferroelectric oxides", 3rd Intern. Symp. on Integrated Ferroelectrics, Colorado Springs, April 1991.

D. M. Smyth, "Defect chemistry of perovskites", Polar Solids Discussion Group: Defects and Electronic Properties of Complex Ceramic Oxides, Oxford University, April 1991.

D. M. Smyth, "The influence of defects on the electrical properties of perovskite and perovskite-related materials", 25th Anniversary Meeting of the Dielectric Society, London, April 1992.

M. V. Raymond and D. M. Smyth, "Defects and transport in PZT", Second CIS- USA Seminar on Ferroelectricity, St. Petersburg, Russia, June 1992.

D. M. Smyth, "Ionic transport in ferroelectrics", Eighth Intern. Meeting on Ferroelectricity, Gaithersburg MD, August 1993.

J. Chen, M. P. Harmer, and D. M. Smyth, "In situ TEM observation of domain boundary motion in ferroelectric materials", Eighth Intern. Meeting on Ferroelectricity, Gaithersburg MD, August 1993.

D. M. Smyth, "Electronic and ionic charge transport in high permittivity materials", 184th Meeting of the Electrochemical Society, New Orleans, October 1993.

C. C. Dong, M. V. Raymond, and D. M. Smyth, "Perovskite defect chemistry revisited", 1993 Pac Rim Meeting, Honolulu, November 1993.

W. L. Warren, D. B. Dimos, B. A. Tuttle, J. Robertson, M. V. Raymond, and D. M. Smyth, "Hole-trapping in ferroelectric oxides", Sixth U.S.-Japan Seminar on Dielectric and Piezoelectric Ceramics, Lahaina, Hawaii, November 1993.

M. V. Raymond and D. M. Smyth, "Nonstoichiometry, defects, and charge transport in PZT", NATO Advanced Research Workshop, Science and Technology of Electroceramic Thin Films, Maratea, Italy, June 1994.

D. M. Smyth, "Nonstoichiometry, doping, and transport in ferroelectric perovskites", Ninth Intern. Symp. on the Applications of Ferroelectrics, The Pennsylvania State University, August 1994.

D. M. Smyth, "Defects and charge transport in perovskite ferroelectrics", Third Williamsburg Workshop on Fundamental Experiments in Ferroelectrics, Williamsburg, VA, February 1995.

D. M. Smyth, "Defect chemistry of PZT thin films", Workshop on Ferroelectric Thin Films, Lausanne, Switzerland, February 1995.

B. Contributed

P. Peng and D. M. Smyth, "Defect chemistry of a self-compensated complex perovskite, $Ba(Zn_{1/3}Nb_{2/3})O_3$, 93rd Annual Meeting of the American Ceramic Society, Cincinnati, April 1991.

M. V. Raymond, P. Peng, and D. M. Smyth, "Defect chemistry analysis of lead-based ferroelectrics", 93rd Annual Meeting of the American Ceramic Society, Cincinnati, April 1991.

M. V. Raymond and D. M. Smyth, "Defect chemistry analysis of the $Pb(Zr_xTi_{1-x})O_3$ system and its application to the degradation of thin film memories", 3rd Intern. Symp. on Integrated Ferroelectrics, Colorado Springs, April 1991.

M. V. Raymond and D. M. Smyth, "Defect chemistry analysis of degradation in $Pb(Zr_xTi_{1-x})O_3$ thin films", 4th Intern. Symp. on Integrated Ferroelectrics, Monterey, CA, March 1992.

J. Chen, M. P. Harmer, and D. M. Smyth, "Polarization degradation in perovskite ferroelectric ceramics and thin films", Eighth Intern. Symp. on the Applications of Ferroelectrics, Gaithersburg, MD, August 1992.

M. V. Raymond, J. Chen, D. M. Smyth, and M. P. Harmer, "Degradation of ferroelectric thin films: A defect chemistry approach", 5th Intern. Symp. on Integrated Ferroelectrics, Colorado Springs, April 1993.

M. V. Raymond and D. M. Smyth, "Defect chemistry and transport properties of $PbZr_xTi_{1-x}O_3$", 5th Intern. Symp. on Integrated Ferroelectrics, Colorado Springs, April 1993.

W. L. Warren, D. M. Smyth, D. Dimos, C. H. Seager, and B. A. Tuttle, "Lead vacancies, Pb^{+3} centers, and optical writing in PZT materials", Eighth Intern. Meeting on Ferroelectricity, Gaithersburg, MD, August 1993.

M. V. Raymond and D. M. Smyth, "Defect chemistry and transport properties of $Pb(Zr_xTi_{1-x})O3$", Fifth Intern. Symp. on Integrated Ferroelectrics, April 1993.

W. L. Warren, B. A, Tuttle, C. H. Seager, and D. M. Smyth, "Transient hole traps in PZT", Eighth Intern. Meeting on Ferroelectricity, Gaithersburg, MD, August 1993.

V. Saikumar, M. P. Harmer, and D. M. Smyth, "In-situ TEM studies of ferroelectric materials", 96th Annual Meeting of the American Ceramic Society, Indianapolis, April 1994.

D. M. Smyth, V. Saikumar, D. Dimos, R. W. Schwartz, and S. J. Lockwood, "Compostional effects on polarization fatigue and leakage currents in PZT", Ninth Intern. Symp. on the Applications of Ferroelectrics, The Pennsylvania State University, August 1994.

C. C. Dong, M. V. Raymond, and D,. M. Smyth, "The insulator-semiconductor transition in perovskite oxides", Electroceramics IV, 4th Intern. Conf. on Electronic Ceramics and Applications, Aachen, September 1994.

V. Saikumar, H. M. Chan, and M. P. Harmer, 52nd Annual Meeting of the Microscopy Society of America, New Orleans, 1994.

VIII. PUBLICATIONS RELATED TO THIS PROGRAM

D. M. Smyth, "Charge motion in ferroelectric thin films", Ferroelectrics $\underline{116}$, 117 (1991).

J. Chen, M. P. Harmer, and D. M. Smyth, "Polarization fatigue in perovskite ferroelectric ceramics and thin films", Proceedings of the Eighth Intern. Symp. on the Applications of Ferroelectrics.

R. Waser and D. M. Smyth, Defect chemistry, conduction, and breakdown mechanism of perovskite-structure titanates", to appear in Ferroelectric Thin Films: Synthesis and Basic Properties, Vol. I, C. Paz de Araujo, J. F. Scott, and G. W. Taylor, eds., Gordon and Breach, 1994. An invited chapter.

M. V. Raymond and D. M. Smyth, "Defects and transport in $Pb(Zr_{1/2}Ti_{1/2})O_3$", Ferroelectrics $\underline{144}$, 129 (1993).

J. Robertson, W. L. Warren, B. A. Tuttle, D. Dimos, and D. M. Smyth, "Shallow Pb^{+3} hole traps in lead zirconate titanate ferroelectrics", Appl. Phys. Lett. $\underline{63}$, 1519 (1993).

M. V. Raymond, J. Chen, and D. M. Smyth, "Degradation of ferroelectric thin films: A defect chemistry approach", Integrated Ferroelectrics $\underline{5}$, 73 (1994).

M. V. Raymond and D. M. Smyth, "Defect chemistry and transport properties of $Pb(Zr1_{1/2}Ti_{1/2})O_3$", Integrated Ferroelectrics $\underline{4}$, 145 (1994).

J. Chen, M. P. Harmer, and D. M. Smyth, "Compositional control of ferroelectric fatigue in perovskite ferroelectric ceramics and thin films", J. Appl. Phys. $\underline{76}$ (9), 5394 (1994).

D. M. Smyth, "Ionic transport in ferroelectrics", Ferroelectrics $\underline{151}$, 115 (1994).

W. L. Warren, J. Robertson, D. Dimos, B. A. Tuttle, and D. M. Smyth, "Transient hole traps in PZT", Ferroelectrics $\underline{153}$, 303 (1994).

C. C. Dong, M. V. Raymond, and D. M. Smyth, "The insulator-semiconductor transition in perovskite oxides", in Electroceramics IV, Proceedings Vol. I, R. Waser, S. Hoffmann, D. Bonnenberg, and Ch. Hoffman, eds., Augustinus Buchhandlung, Aachen 1994, p.47.

M. V, Raymond and D. M. Smyth, "Nonstoichiometry, defects, and charge transport in PZT", to appear in Science and Technology of Electroceramic Thin Films, O Auciello and R. Waser, eds., Kluwer Academic Press, Amsterdam (1995).

M. V. Raymond and D. M. Smyth, "Defects and charge transport in perovskite ferroelectrics", to be submitted to J. Phys. Chem. Solids.

IX. FIGURE CAPTIONS

1. The equilibrium electrical conductivity of $BaTiO_3$ as a function of temperature and oxygen activity. The isotherms are at 50°C intervals.

2. The equilibrium electrical conductivity of $Pb(Zr_{1/2}Ti_{1/2})O_3$ (PZT) as a function of temperature and oxygen activity. Only relatively oxidizing conditions are shown.

3. A schematic diagram of the equilibrium defect concentrations in $BaTiO_3$ as a function of oxygen activity. Only the free electron and hole concentrations are shown.

4. A schematic diagram of the equilibrium defect concentrations in PZT as a function of oxygen activity. The concentration of trapped holes has been included.

5. A schematic diagram of the sealed cell used for the measurement of the equilibrium oxygen activity as a function of temperature at constant defect concentrations.

6. The equilibrium oxygen activity of PZT in the p-type region as a function of temperature at constant defect concentrations.

7. Arrhenius plots of the normalized Seebeck coefficient for acceptor-doped PZT measured in different oxygen activities. The normalized coefficient is proportional to the log of the carrier concentration.

8. A schematic diagram of the sealed cell used for the measurement of the conductivity as a function of temperature at constant defect concentrations.

9. The electrical conductivity of PZT in the p-type region as a function of temperature at constant defect concentrations.

10. The electrical conductivity of $BaTiO_3$ quenched after equilibration with various oxygen activities at 800 or 1000°C. The bulk conductivity was obtained by ac impedance analysis.

11. The electrical conductivity of PZT quenched after equilibration with various oxygen activities at 700°C. The bulk conductivity was obtained by ac impedance analysis.

12. The electrical conductivity of PZT quenched after equilibration in a highly reducing atmosphere at 700°C. The bulk conductivity was obtained by ac impedance analysis.

13. A schematic diagram of the equilibrium defect concentrations in PZT as a function of oxygen activity. A hypothetical line for the concentration of trapped electrons has been included.

14. The normalized remanent polarization for thin, polycrystalline BaTiO$_3$ as a function of the number of unipolar switching cycles. Results for undoped, acceptor-doped, and donor-doped samples are shown.

15. The normalized remanent polarization for undoped and donor-doped PZT thin films as a function of the number of bipolar switching cycles.

16. Defect concentrations as a function of donor concentration for PZT in which the acceptor impurity content exceeds the amount of PbO-loss.

17. Defect concentrations as a function of donor concentration for PZT in which the amount of PbO-loss exceeds the acceptor impurity content.

18. A schematic diagram of the field stage in which an electric field can be applied to a thinned sample in the transmission electron microscope.

19. The electrode configuration applied to the thinned samples.

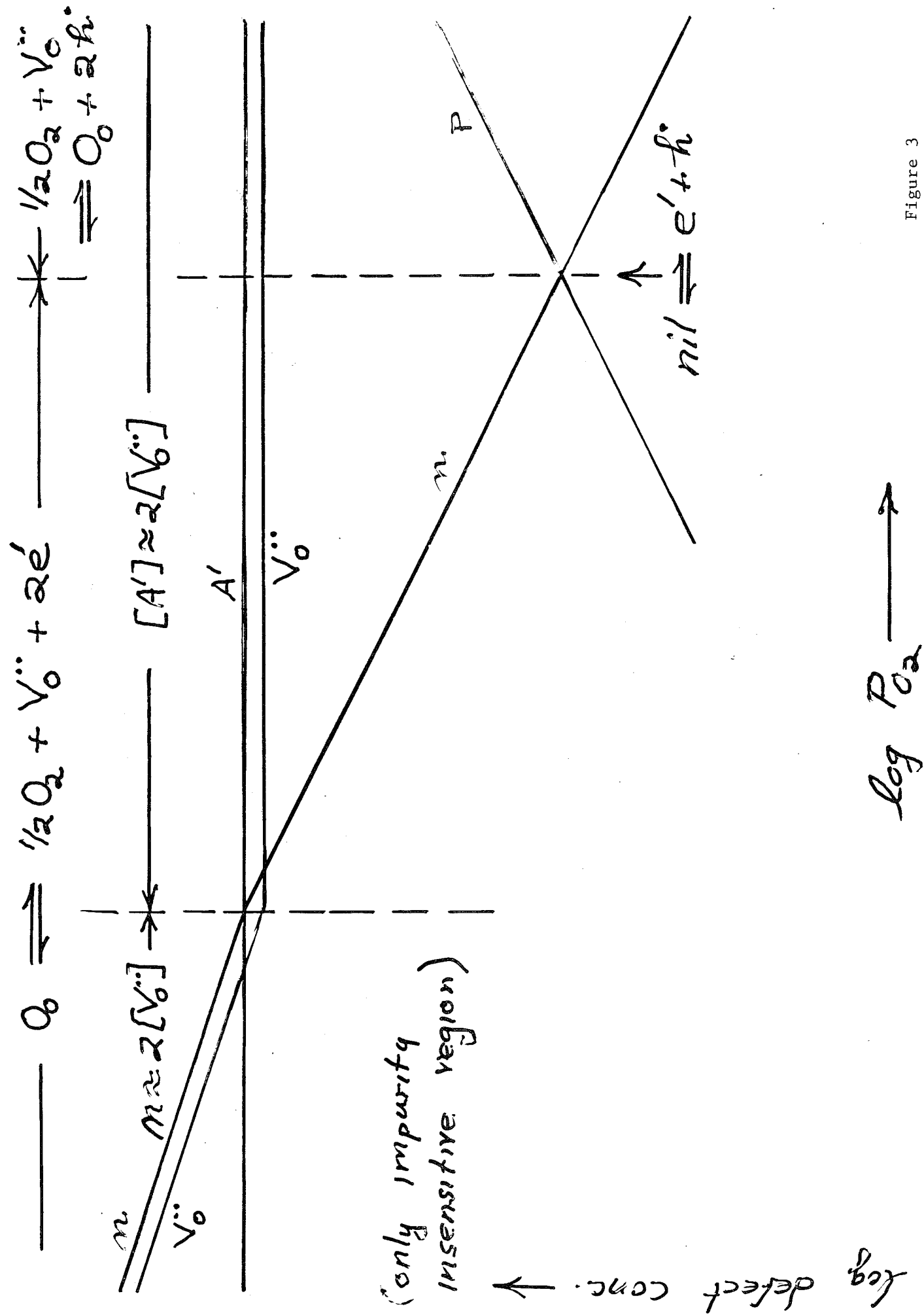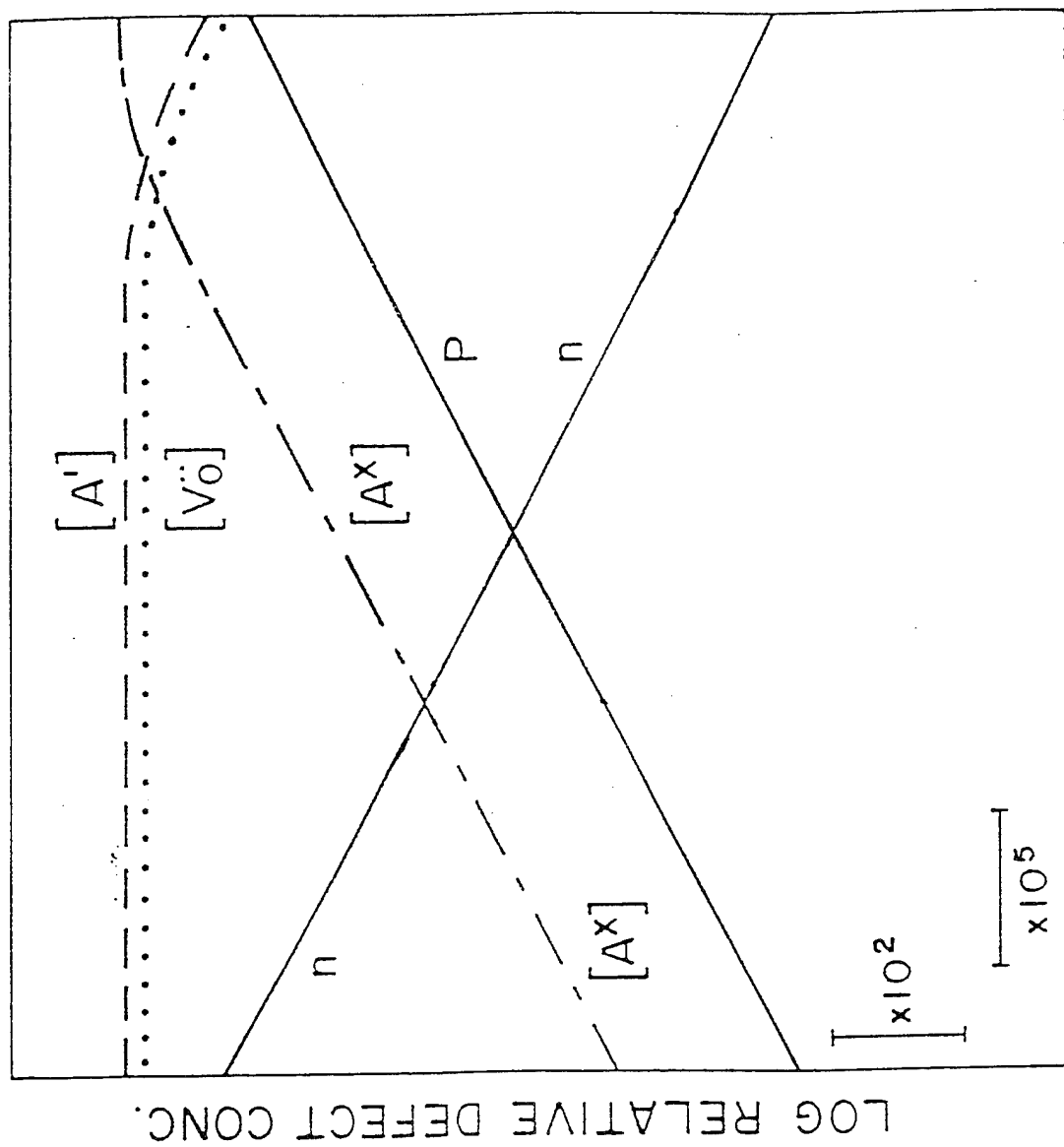N.-H. Chan and D.M. Smyth, J. Electrochem. Soc., 123 [10] 1584 (1976)

134 ppm Al-doped BaTiO₃
Ba/Ti = 0.995

Log Conductivity (ohm⁻¹ cm⁻¹)

Log P(O₂) (atm.)
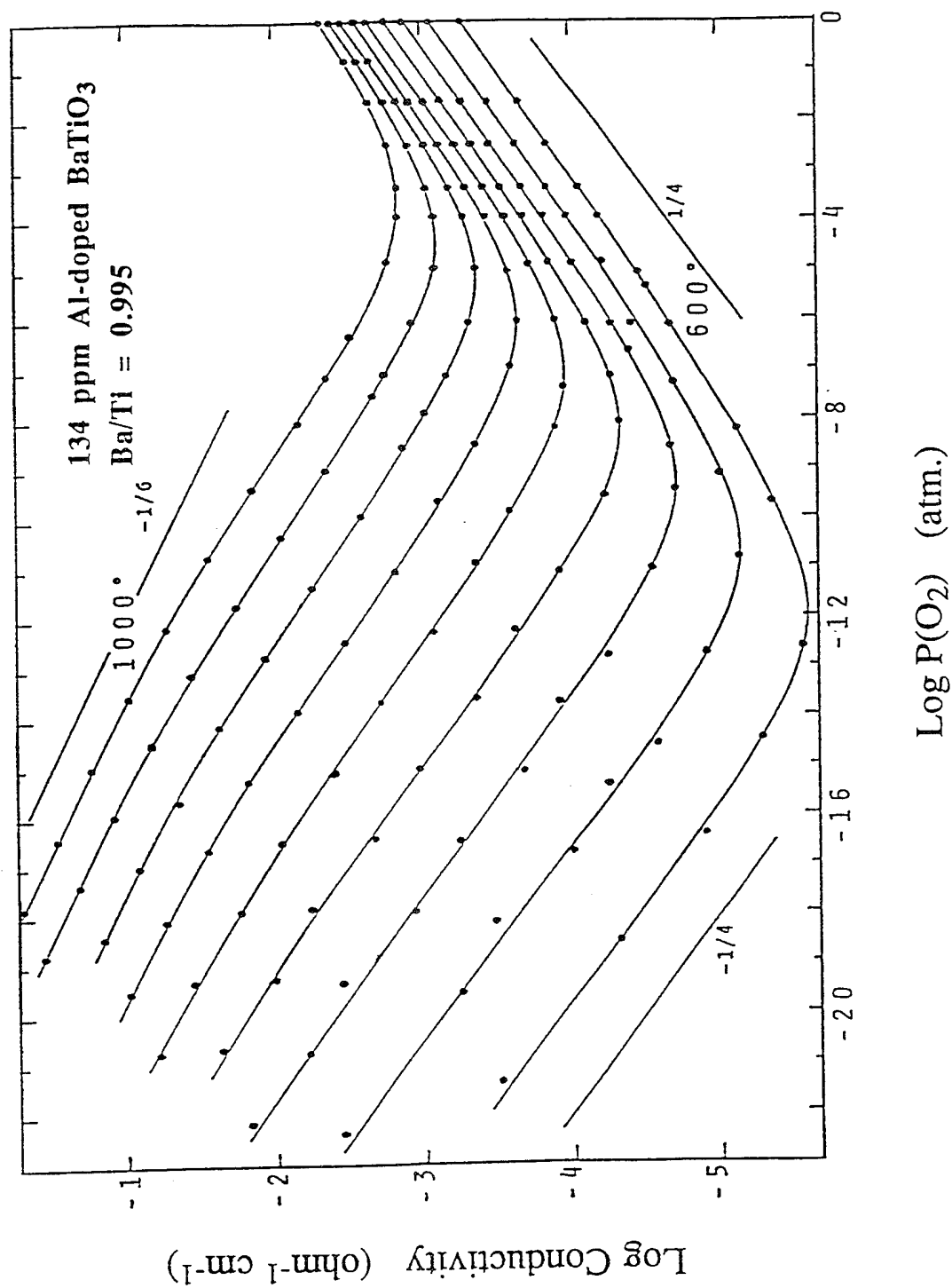
Figure 1

Figure 2

Figure 3

Axis labels: $\log$ defect conc. ; $\log P_{O_2}$

$\frac{1}{2}O_2 + V_0^{\cdot\cdot} \rightleftharpoons O_0 + 2h^{\cdot}$

$O_0 \rightleftharpoons \frac{1}{2}O_2 + V_0^{\cdot\cdot} + 2e'$

$nil \rightleftharpoons e' + h^{\cdot}$

$[A'] \approx 2[V_0^{\cdot\cdot}]$

$n \approx 2[V_0^{\cdot\cdot}]$

A', $V_0^{\cdot\cdot}$, n, p

(only impurity insensitive region)

Figure 4

Yittria stabilized Zirconia electrolyte with Pt electrodes and leads

PZT specimen

Alumina ring, tube, and disk

Glass rings
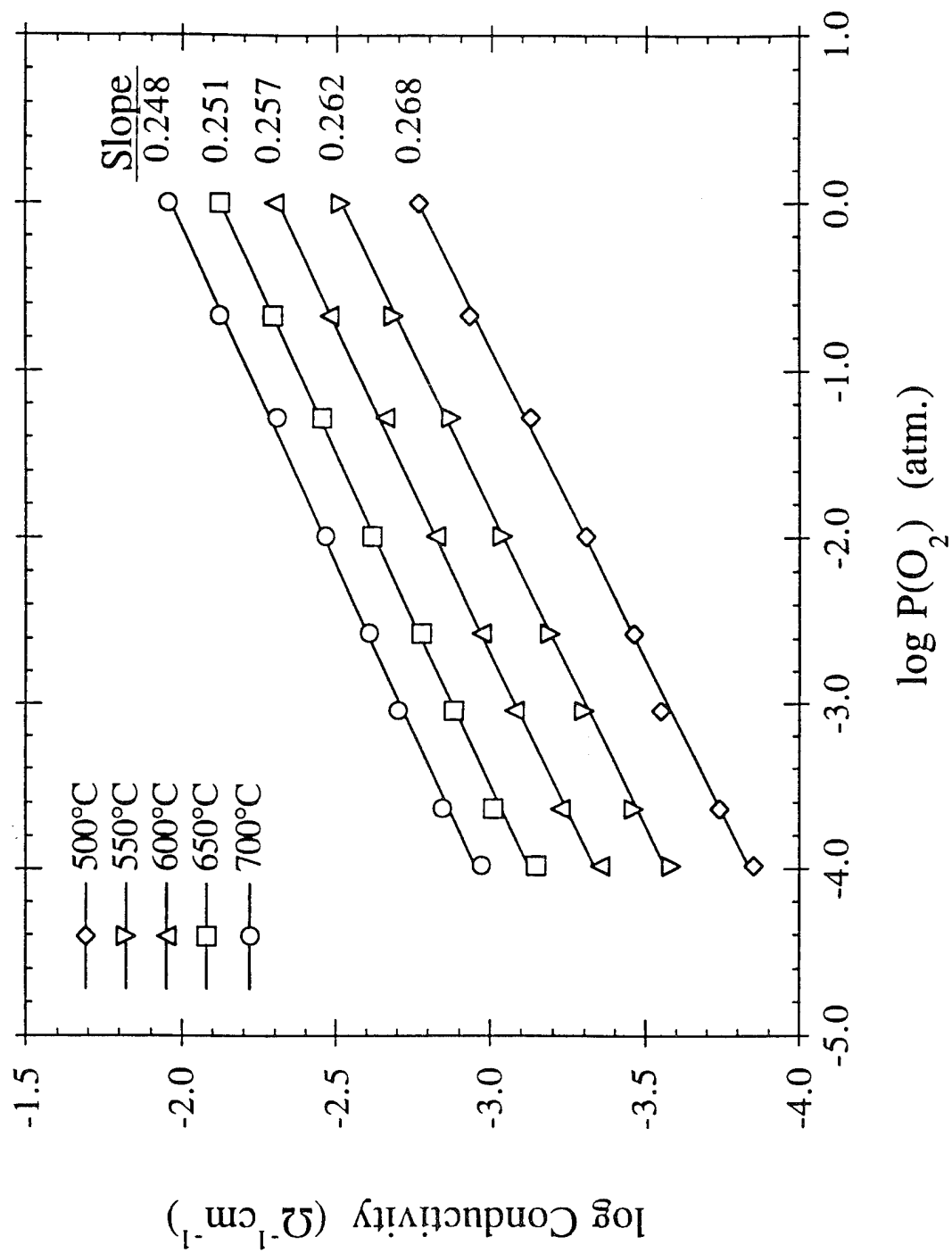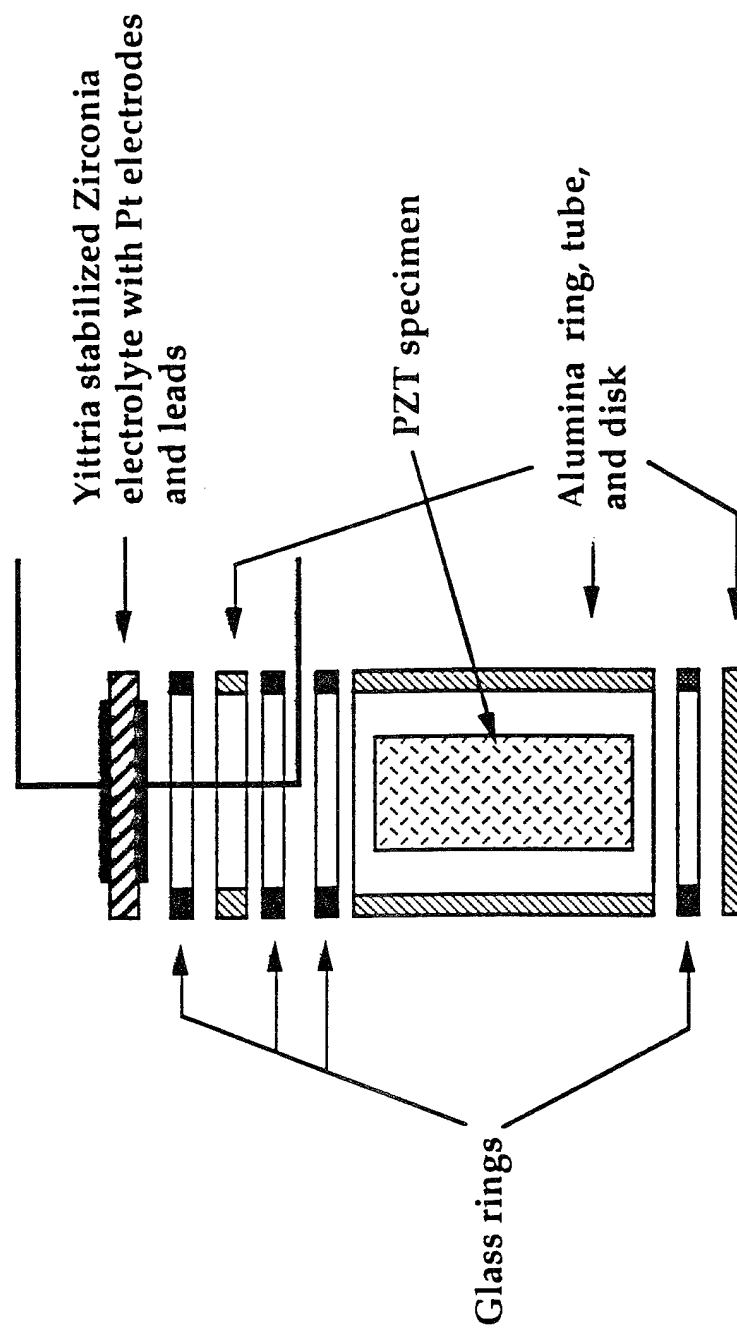
Figure 5

Constant composition oxygen activity measurement for PZT

$\Delta H_{ox} = -0.49$ eV

$\text{Log P(O}_2)$ (atm)

$1000/\text{T}$ (K^{-1})
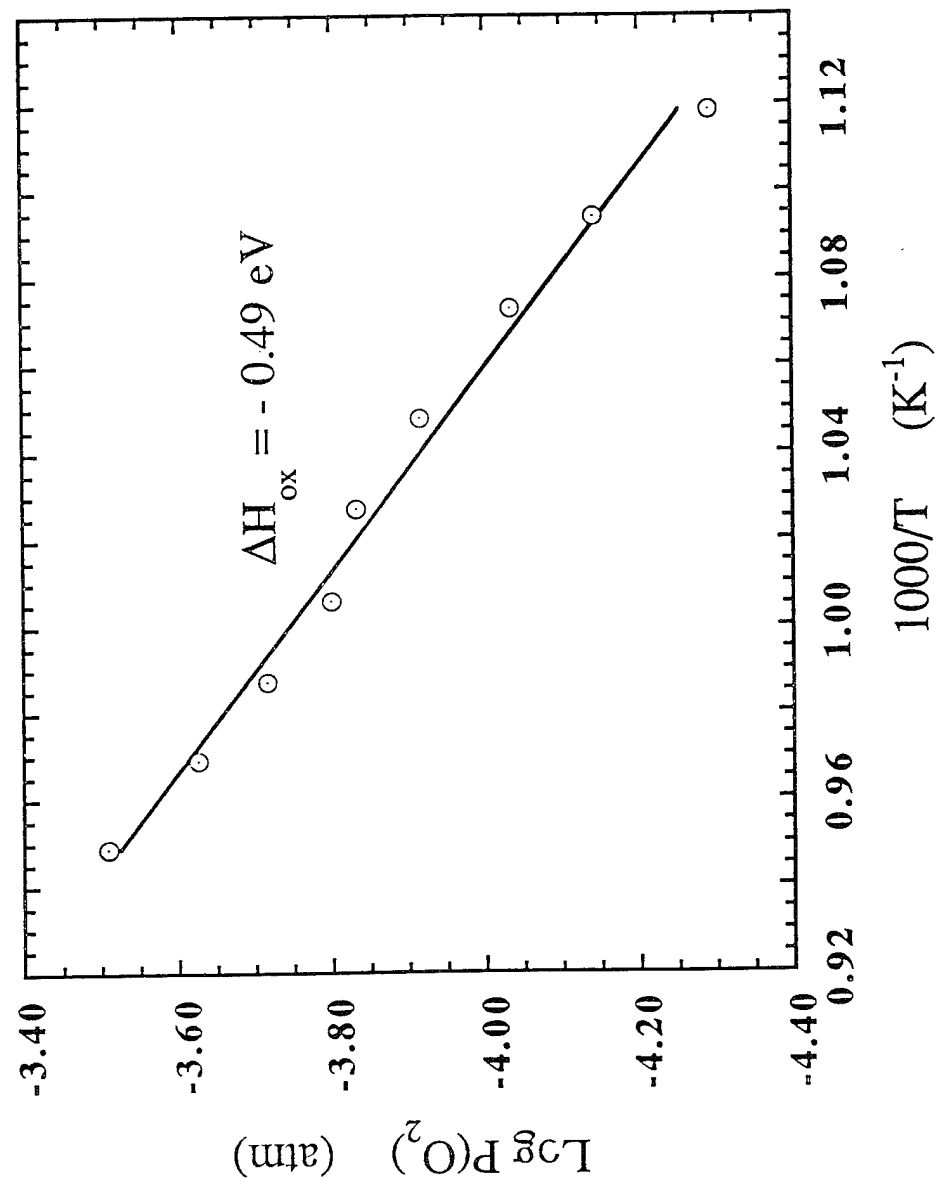
Figure 6

Arrhenius plot of $-eQ/2.3k_B$ for 0.8 at% Al-doped PZT, sinter lot F-036B

0.46 eV

$\Delta H_{ox}/2 + E_A$ = energy

0.52 eV

0.65 eV

Log $P(O_2)$

● 0.0 atm

■ -1.85 atm

▲ -4.3 atm

1000/T (1/K)

$-eQ/2.303k_B$
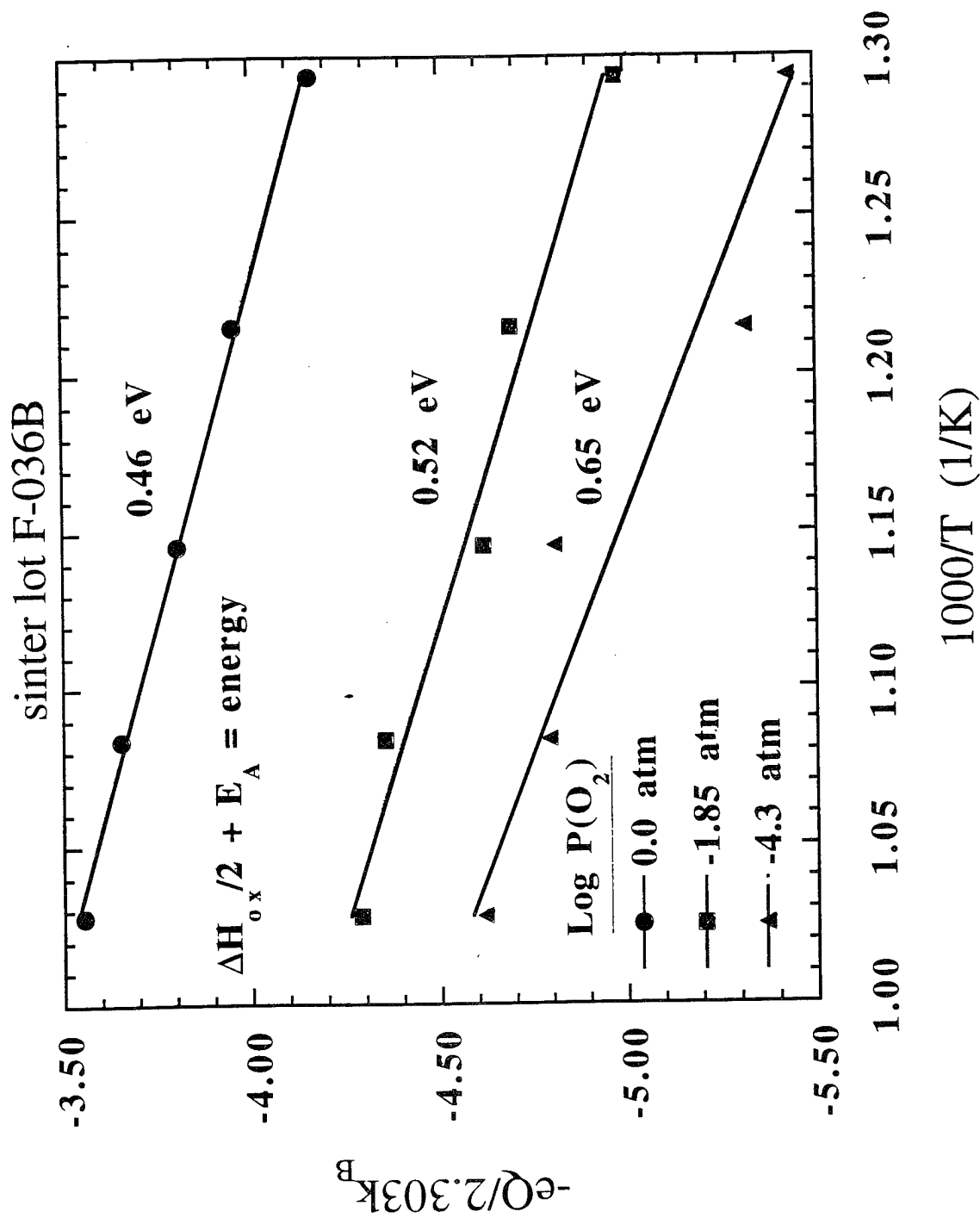
Figure 7

Constant composition conductivity cell diagram

Yittria stabilized
Zirconia electrolyte with
Pt electrodes and leads

Alumina ring
and tube

PZT specimen
with Pt leads

Machinable alumina with
feed through holes to be
sealed with a soft glass
(Tsoft ≈ 450 - 600C)

Glass rings
Tsoft = 717 C

Pt wires (4)
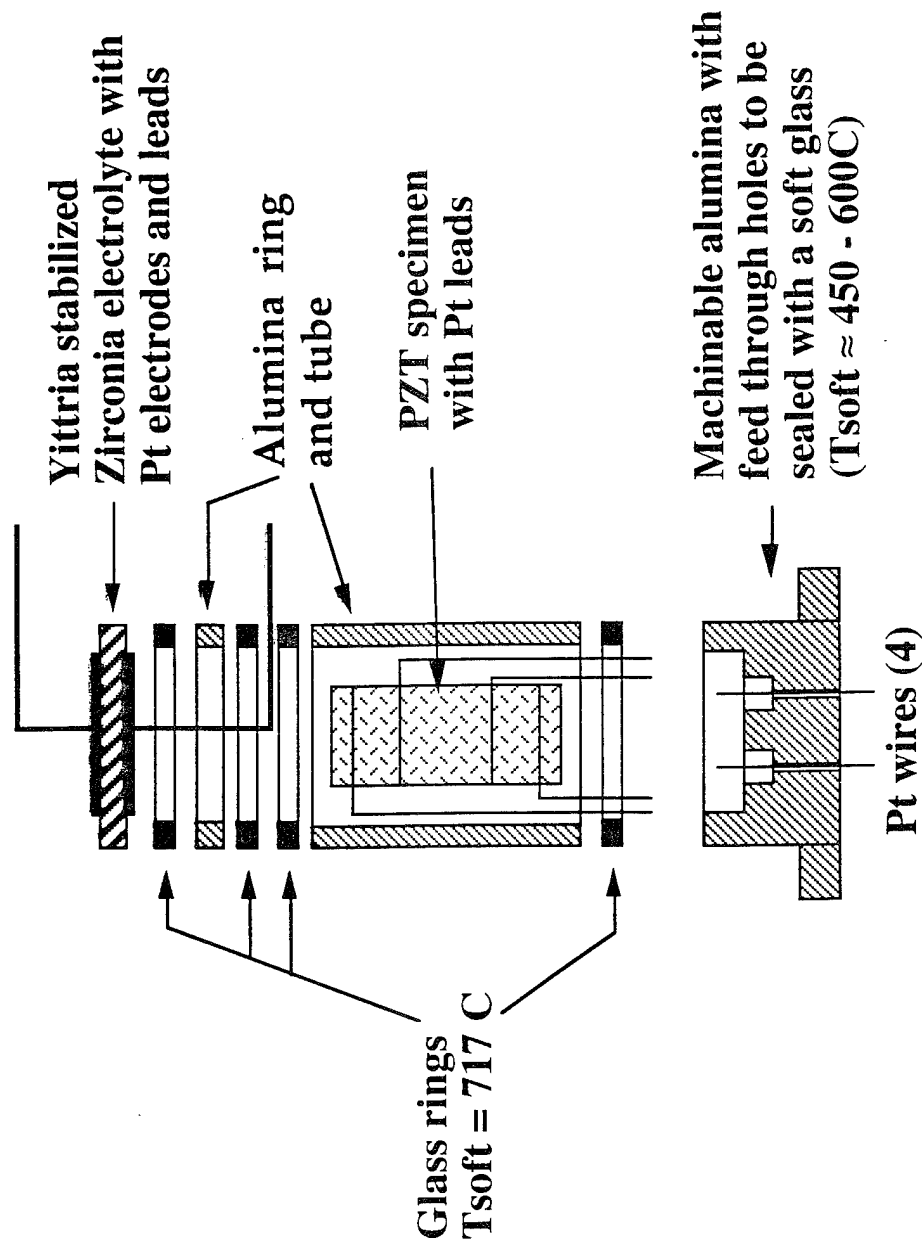
Figure 8

Arrhenius plot of constant composition conductivity for PZT, sinter lot F-007B

$E_A + \Delta H_m = 0.98$ eV

Log (Conductivity$_{(cc)}$ *T) (ohm^{-1}- cm^{-1}- K)

1000/T (K^{-1})
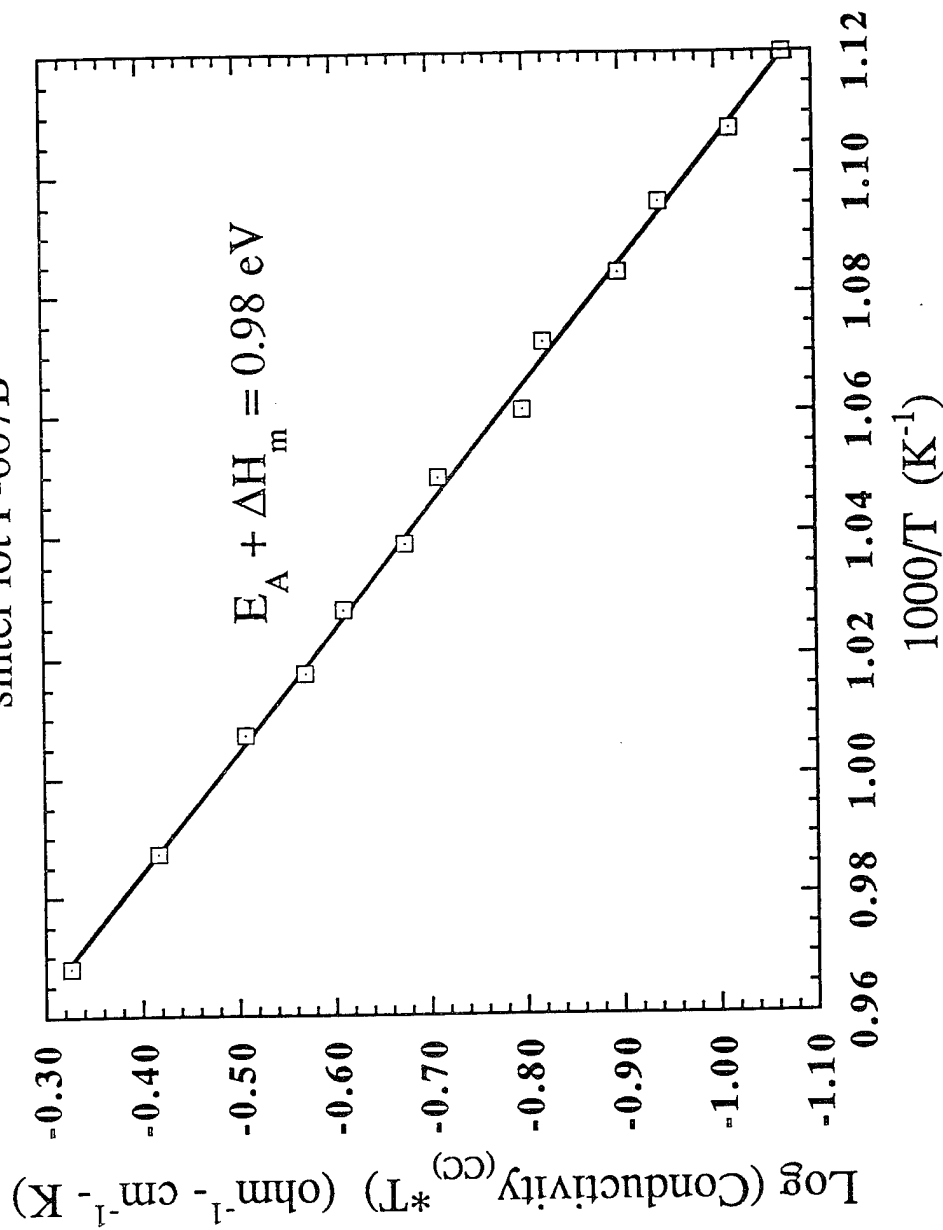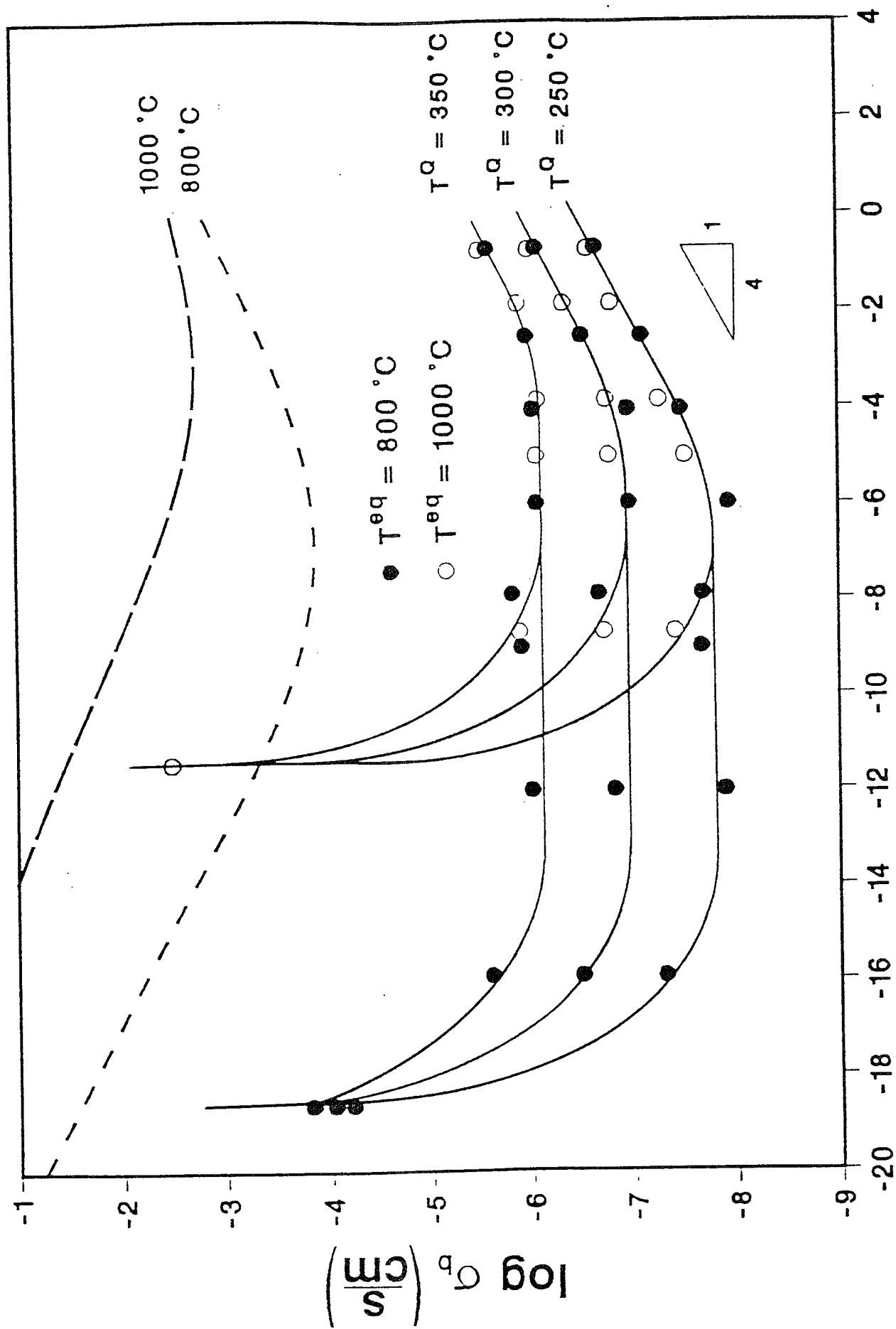
Figure 9

Figure 10

AC conductivity of high purity, undoped PZT quenched from various $P(O_2)$'s at 700°C.
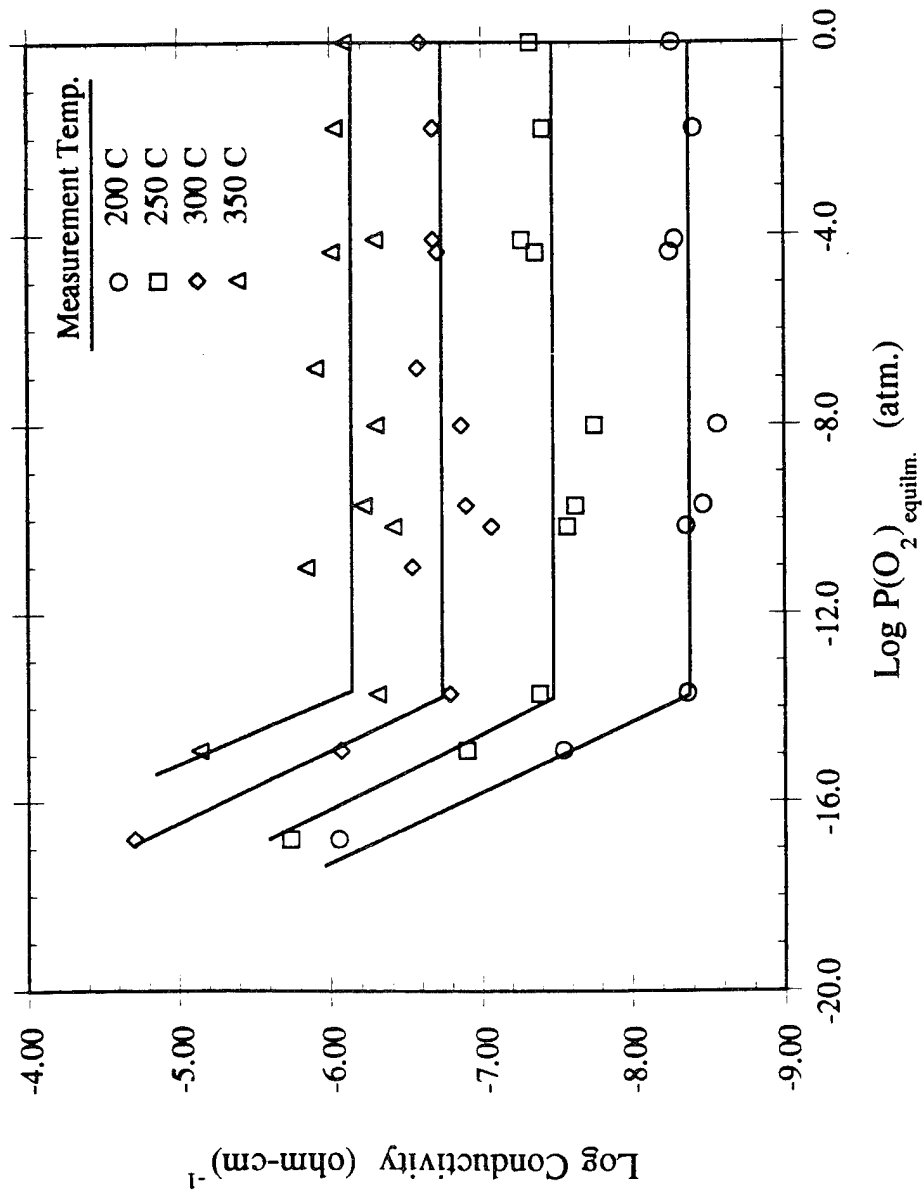
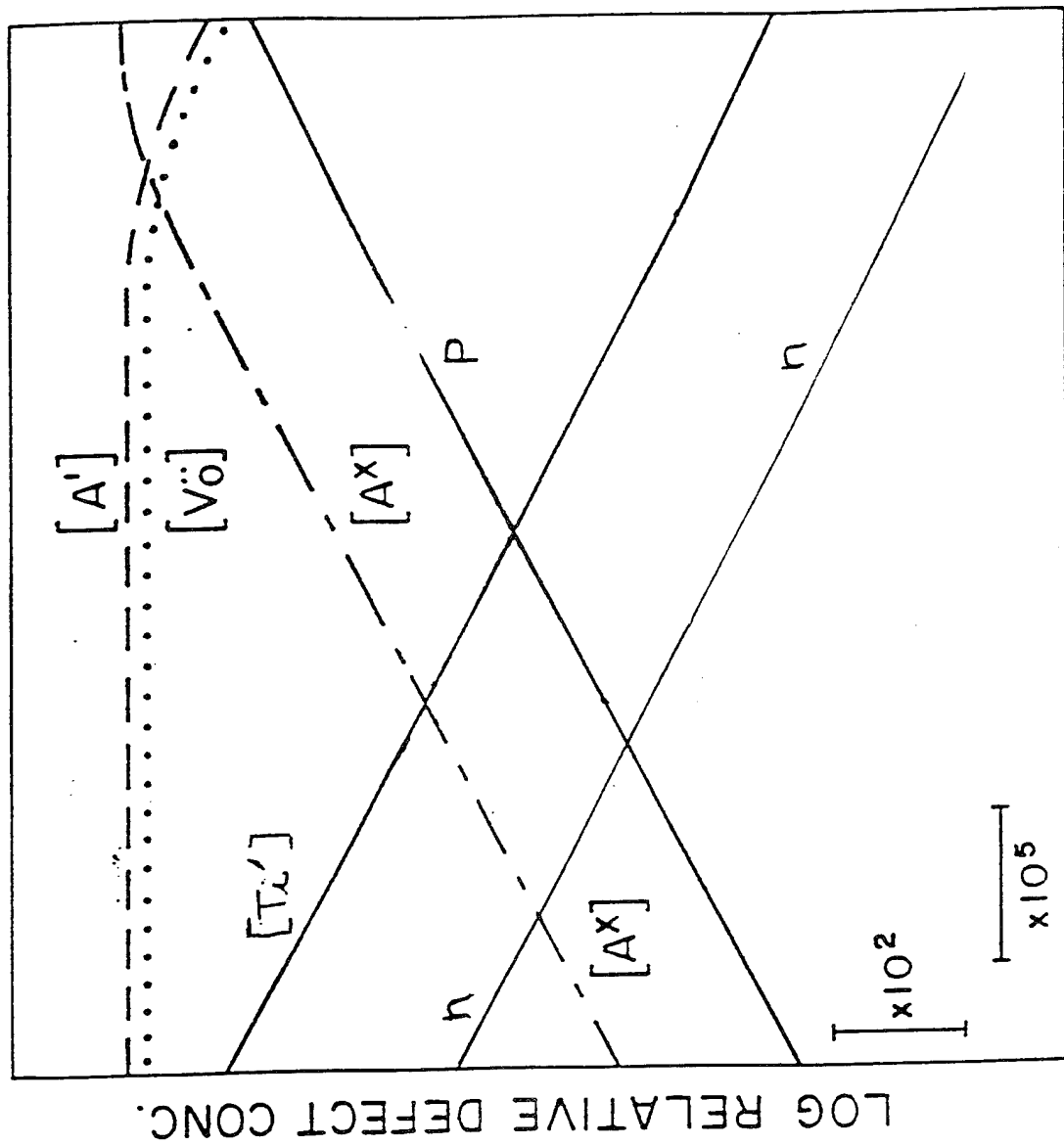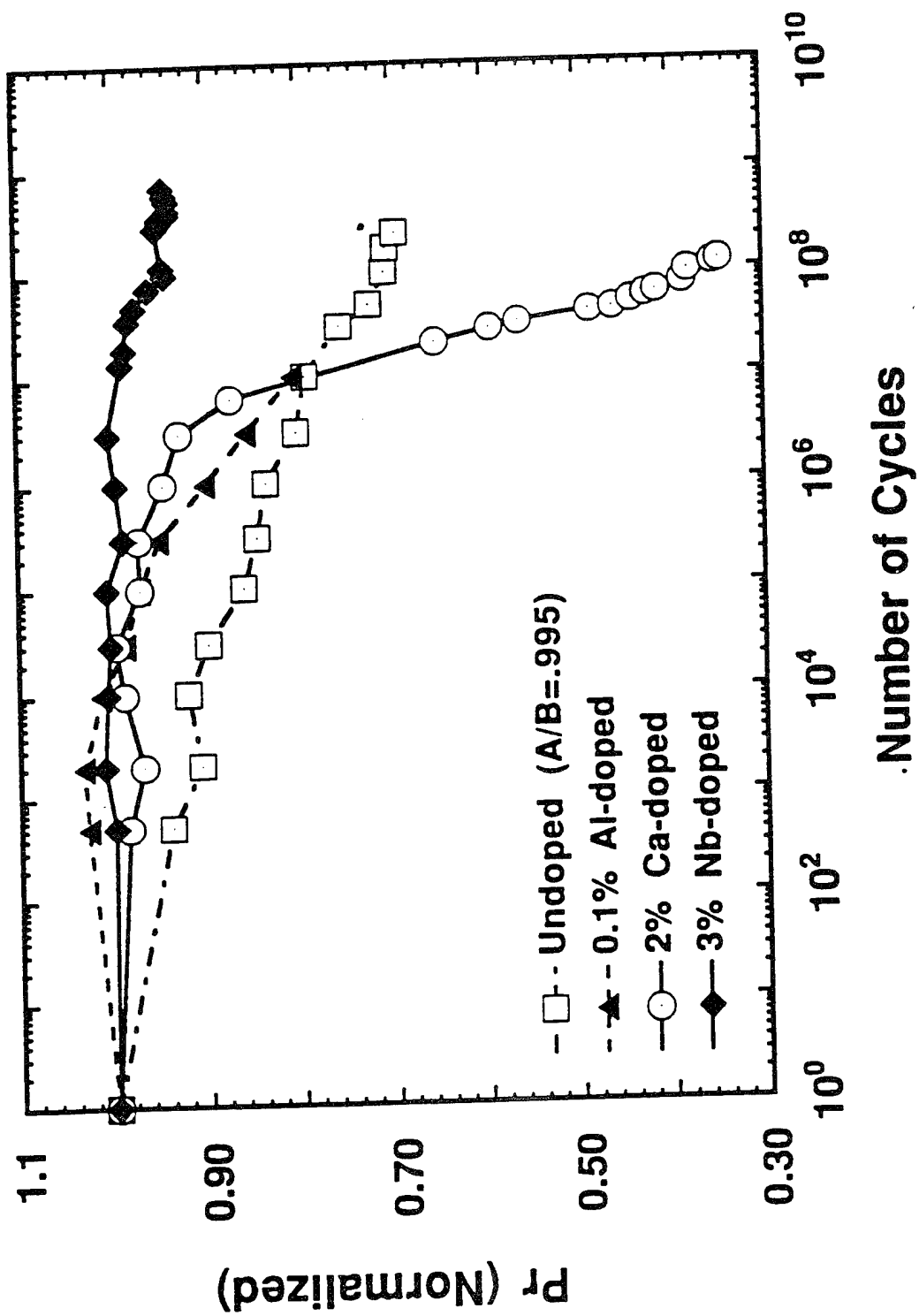Figure 11
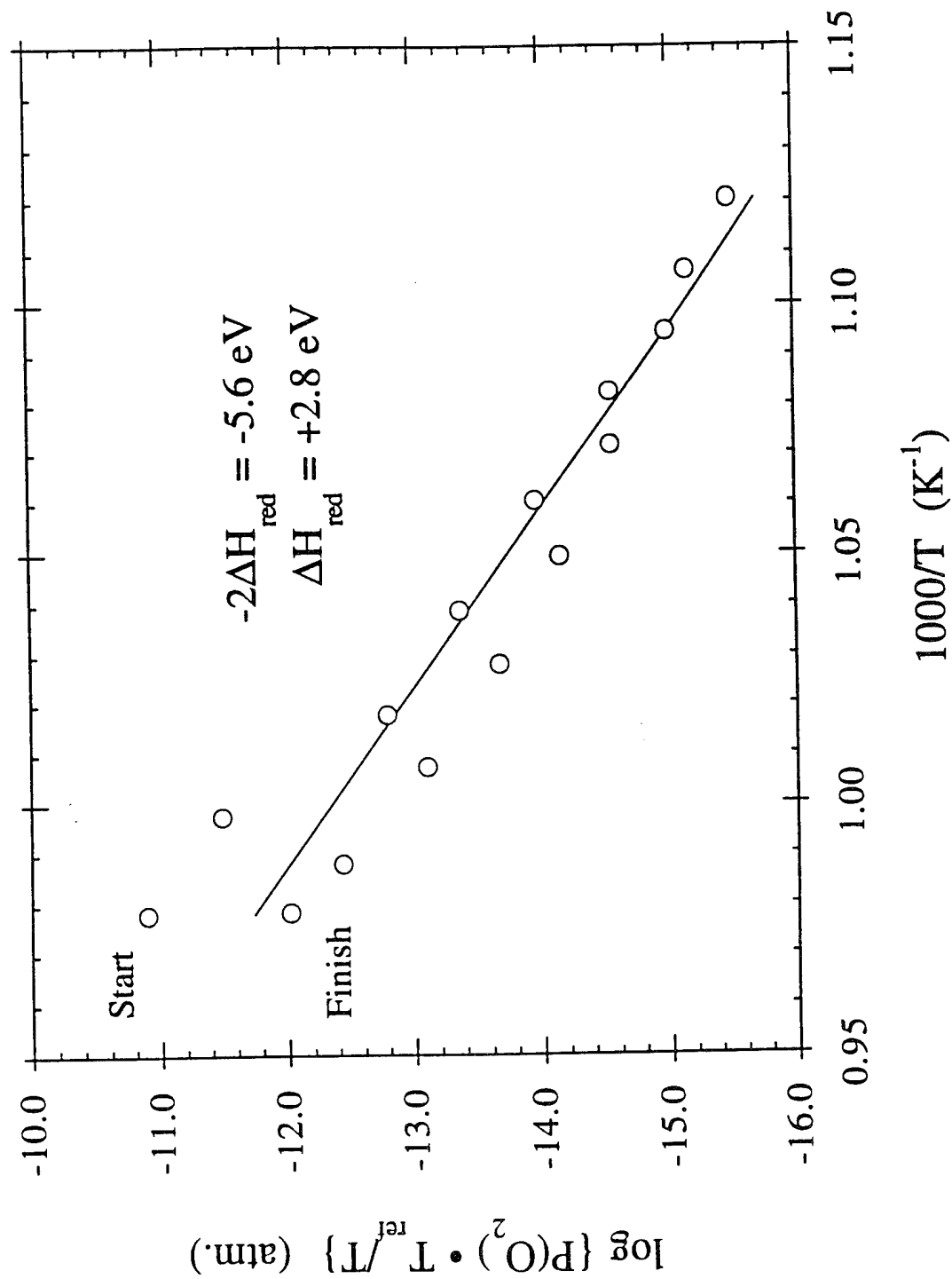
Figure 12

Figure 13

Figure 14
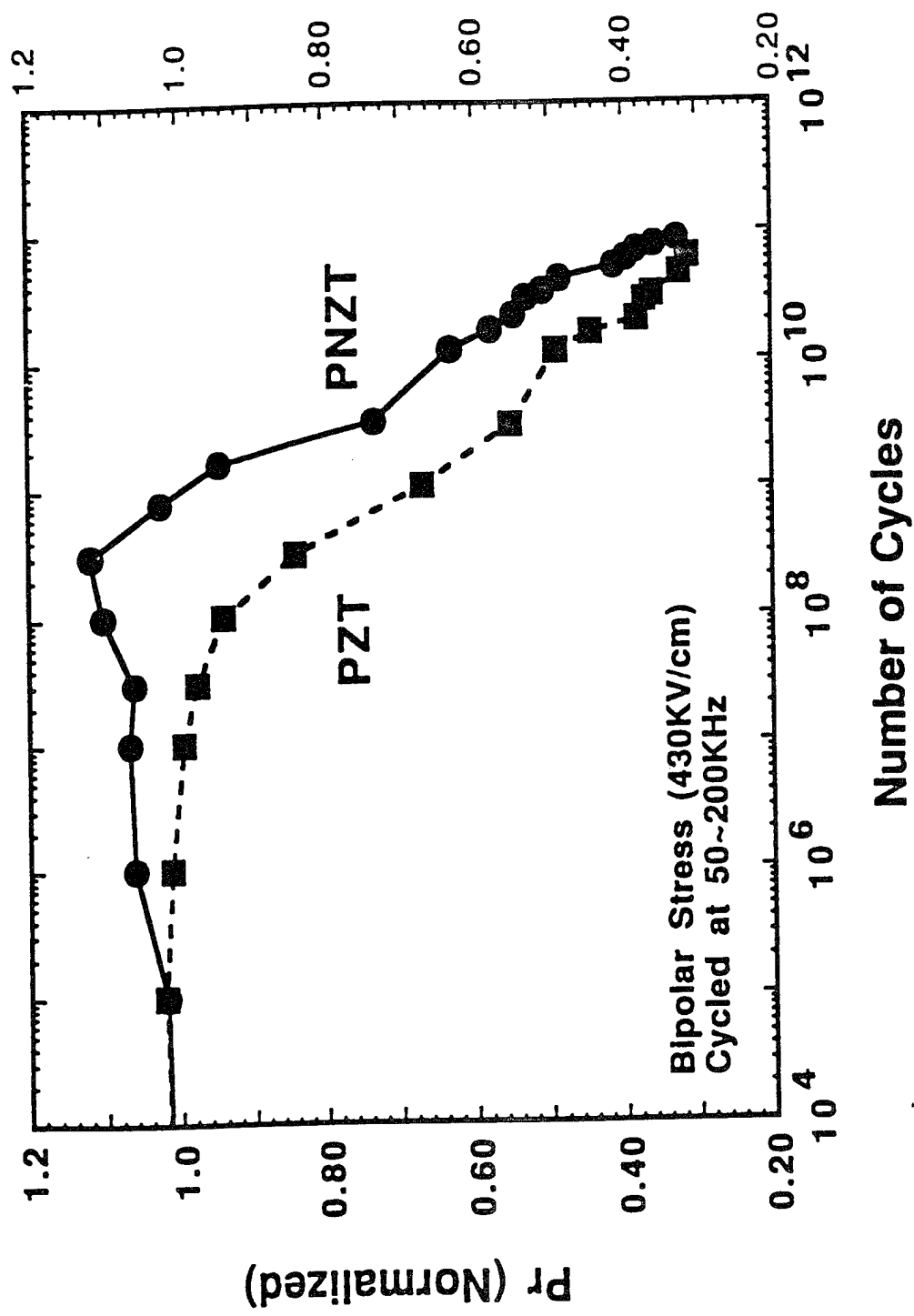
Figure 15

Figure 16

Figure 17

Modified TEM Single Tilt Heating Stage

front surface electrical contact

alumina ring with electrical contacts

evaporated Au electrodes

BaTiO3 thin foil

heater coils

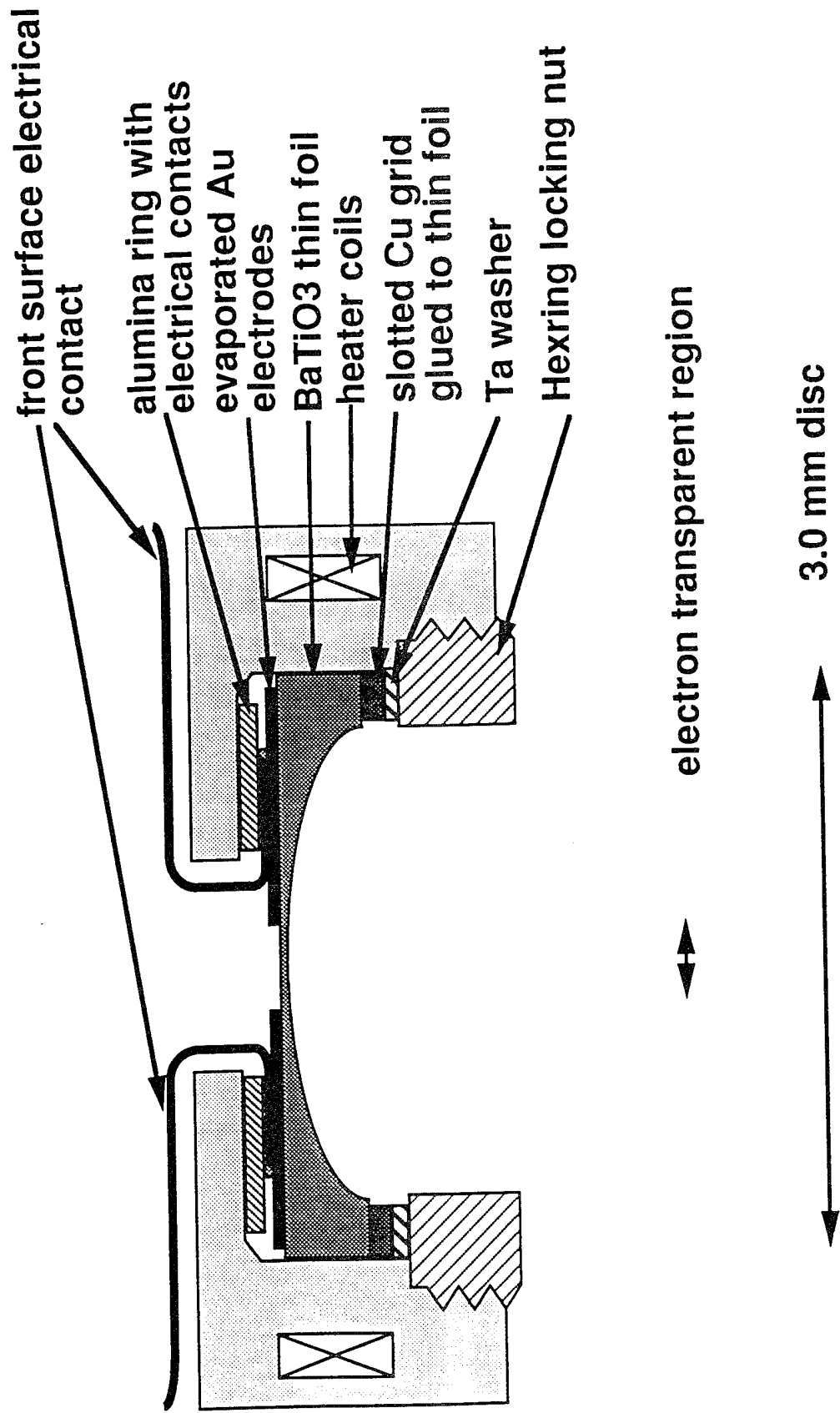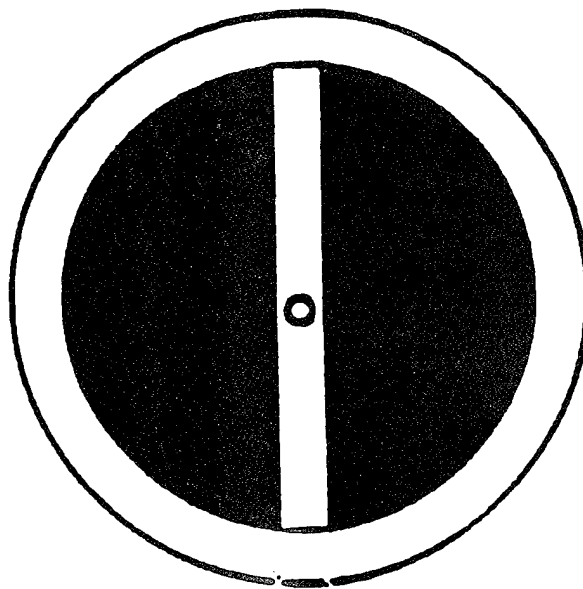slotted Cu grid glued to thin foil

Ta washer

Hexring locking nut

electron transparent region

3.0 mm disc

Figure 18

42 μm

Figure 19